Development 126, 3831-3846 (1999)
Printed in Great Britain © The Company of Biologists Limited 1999
DEV4175

Dlx5 regulates regional development of the branchial arches and sensory capsules

Michael J. Depew[1,*], Jen Kuei Liu[1,*,‡], Jason E. Long[1,*], Robert Presley[2], Juanito J. Meneses[3], Roger A. Pedersen[3] and John L. R. Rubenstein[1,§]

[1]Nina Ireland Laboratory of Developmental Neurobiology, Center for Neurobiology and Psychiatry, Department of Psychiatry and Programs in Neuroscience, Developmental Biology, Oral Biology and Biomedical Sciences, 401 Parnassus Avenue, University of California at San Francisco, S.F., CA, 94143-0984, USA
[2]Anatomy Unit, University of Wales, Cardiff, UK
[3]Reproductive Genetics Unit, Department of Obstetrics, Gynecology and Reproductive Sciences, University of California at San Francisco, S.F., CA, 94143, USA
*Joint first authors
‡Present address: Sentinel Biosciences, 855 South California Avenue, Suite C, Palo Alto CA 94304, USA
§Author for correspondence (email: jlrr@cgl.ucsf.edu)

Accepted 31 May; published on WWW 5 August 1999

SUMMARY

We report the generation and analysis of mice homozygous for a targeted deletion of the *Dlx5* homeobox gene. *Dlx5* mutant mice have multiple defects in craniofacial structures, including their ears, noses, mandibles and calvaria, and die shortly after birth. A subset (28%) exhibit exencephaly. Ectodermal expression of *Dlx5* is required for the development of olfactory and otic placode-derived epithelia and surrounding capsules. The nasal capsules are hypoplastic (e.g. lacking turbinates) and, in most cases, the right side is more severely affected than the left. Dorsal otic vesicle derivatives (e.g. semicircular canals and endolymphatic duct) and the surrounding capsule, are more severely affected than ventral (cochlear) structures. *Dlx5* is also required in mandibular arch ectomesenchyme, as the proximal mandibular arch skeleton is dysmorphic. *Dlx5* may control craniofacial development in part through the regulation of the *goosecoid* homeobox gene. *goosecoid* expression is greatly reduced in *Dlx5* mutants, and both *goosecoid* and *Dlx5* mutants share a number of similar craniofacial malformations. *Dlx5* may perform a general role in skeletal differentiation, as exemplified by hypomineralization within the calvaria. The distinct focal defects within the branchial arches of the *Dlx1*, *Dlx2* and *Dlx5* mutants, along with the nested expression of their RNAs, support a model in which these genes have both redundant and unique functions in the regulation of regional patterning of the craniofacial ectomesenchyme.

Key words: Branchial arch, *Dlx5*, Placode, Mouse, Craniofacial defect

INTRODUCTION

The mammalian skull is an assemblage of skeletal elements with diverse developmental origins which encases the brain, its associated primary sensory organs (olfactory, visual, auditory, vestibular and gustatory), and the oral and respiratory cavities. The embryologically earliest skeletal structures to appear are the cartilaginous (chondrocranial) elements whose development appears to reflect the ancient bauplan of the vertebrate skull (Goodrich, 1958; Youssef, 1966; Barghusen and Hopson, 1979; Moore, 1981; De Beer, 1985; Zeller, 1987; Thorogood, 1988; Hanken and Thorogood, 1993; Novacek, 1993; Kuratani et al., 1997). Historically, two chondrocranial components have been distinguished: the first is the neurocranium, the skeleton built around the nose, eye, inner ear and base of the brain, and the second is the splanchnocranium, the skeleton of the branchial arches. While most of these structures undergo endochondral ossification, some undergo regression and/or non-osseous replacement. The development of the embryonic chondrocranium is coordinated with the development of the dermatocranium, the later-forming cranial skeleton, which undergoes intramembranous ossification over the brain and adjacent to the surfaces of many chondrocranial elements.

Experimental evidence suggests that both mesenchyme and ectoderm play key roles in controlling of the number, shape, size and differentiation of the cranial anlagen (Noden, 1983, 1991; Hall, 1991; Hanken and Hall, 1993; Thorogood, 1993; Francis-West et al., 1998). Fate-mapping studies in amphibians and birds indicate that the dermatocranium and splanchnocranium ossify from cranial neural crest (CNC)-derived mesenchyme (ectomesenchyme) (Le Douarin, 1982; Noden, 1983, 1991; Hall, 1988; Serbedzija et al., 1992; Couly et al., 1993; Osumi-Yamashita et al., 1994; Köntges and Lumsden, 1996). This evidence further suggests that the CNC produces the mesenchyme that forms the rostral neurocranium:

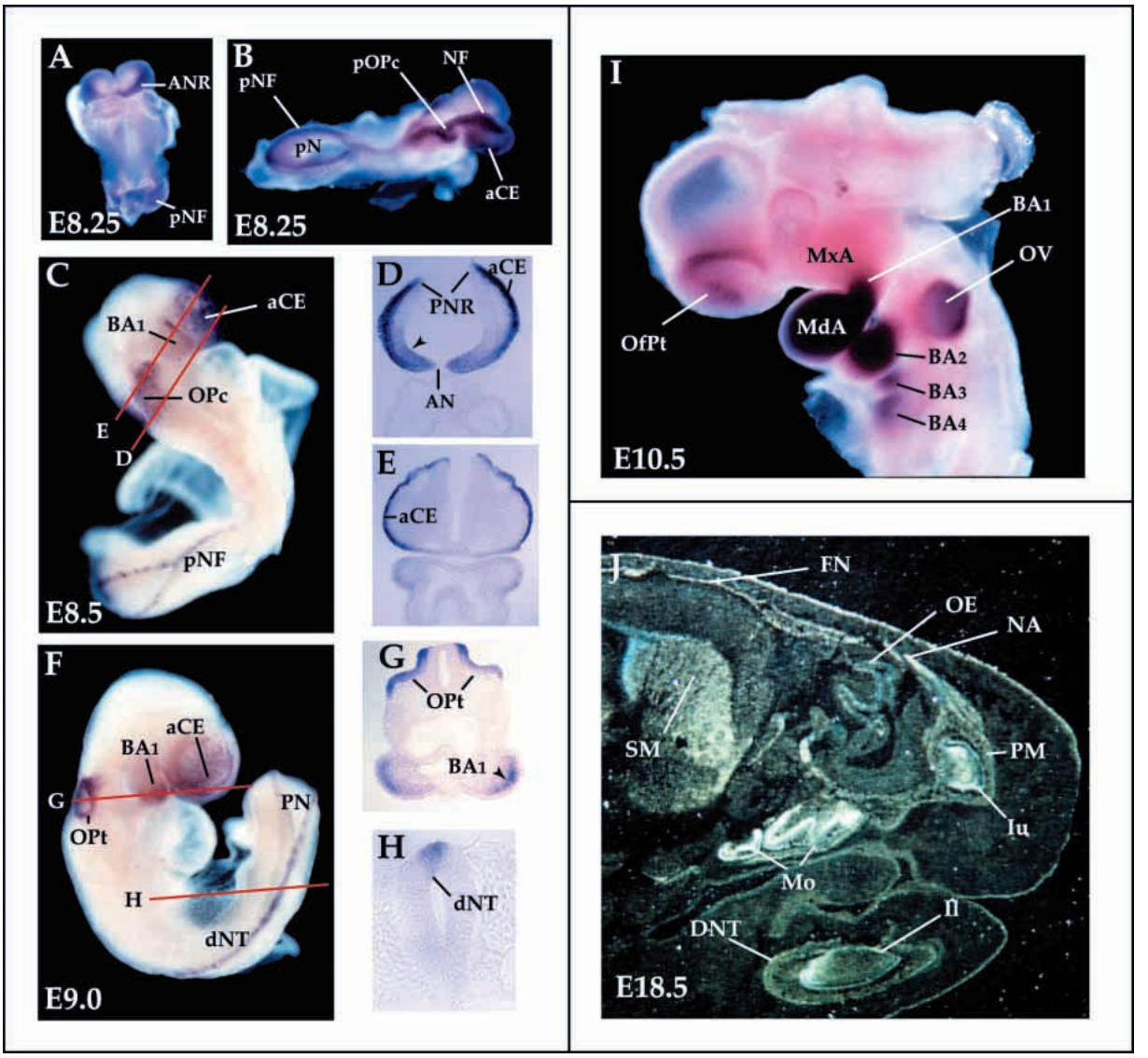

Fig. 1. Expression of murine *Dlx5* from E8.25 to E18.5 revealed by in situ hybridization. (A) Frontal view of an E8.25 (2-somite) embryo shows *Dlx5* expression in the anterior neural ridge (ANR). (B) Dorsolateral view shows expression at E8.25 (4-somite) in the anterior cephalic ectoderm (aCE), the neural fold (NF) and the presumptive otic placode (pOPc). (C) Expression at E8.5 is detectable in the aCE, pNF, otic placode (OPc) and first branchial arch (BA1). (D,E) 8 μm sections of the embryo in C along the planes depicted by the red lines. (D) Expression in the aCE; weaker expression is detected in the anterior prosencephalon (black arrowhead) bordering the anterior neuropore (AN). (E) Expression in the aCE. (F) At E9.0, transcripts are detectable in the otic pit (OPt), aCE, PN, dorsal neural tube (dNT) and ectomesenchyme of BA1. (G,H) 8 μm sections of the embryo in D along the planes depicted by the red lines. (G) Expression is seen in the ectoderm of the entire OPt (though it is strongest at the dorsal margin) and the distal ectomesenchyme of BA1 (black arrowhead). While expression in the dNT (roof plate) is no longer detectable at this axial level, *Dlx5* continues to be expressed at more caudal levels (H). (I) At E10.5, expression is strong within the ectomesenchyme of the branchial arches and the otic vesicle (OV). Cephalic ectodermal expression has become restricted to the internal epithelium of the medial and lateral frontonasal processes surrounding the olfactory pit (OfPt). (J) Radiolabeled in situ hybridization at E18.5 reveals *Dlx5* expression in the forebrain (striatum, SM), olfactory epithelium (OE) and craniofacial hard tissues, including the developing dentary (DNT), premaxilla (PM), frontal (FN), nasal (NA), molars (Mo) and incisors (Il, Iu). Abbreviations: aCE, anterior cephalic ectoderm; AN, anterior neuropore; ANR, anterior neural ridge; BA1, first branchial arch; BA2, second branchial arch; BA3, third branchial arch; BA4, fourth branchial arch; dNT, dorsal neural tube; DNT, dentary; FN, frontal; Il, lower incisor; Iu, upper incisor; MdA, mandibular arch; Mo, molars; MxA, maxillary arch; NA, nasal bone; NF, neural fold; OE, olfactory epithelium; OfPt, olfactory pit; OPc, otic placode; OPt, otic pit; OV, otic vesicle; PM, premaxilla; pN, posterior neuropore; pNF, posterior neural fold; PNR, prosencephalic neural ridge; pOPc, presumptive otic placode; SM, striatum.

the nasal capsules, orbital cartilages and cranial base anterior to the pituitary (trabecular plate cartilage).

Patterning and differentiation of ectomesenchyme is regulated by adjacent epithelial tissues (Mina and Koller, 1987; Lumsden, 1988; Hall, 1991; Thorogood, 1993; Webb and Noden, 1993; Thesleff et al., 1995; Helms et al., 1997; Neubüser et al., 1997; Thesleff and Sharpe, 1997; Tucker et al., 1998, 1999; Hu and Helms, 1999). Specialized thickenings

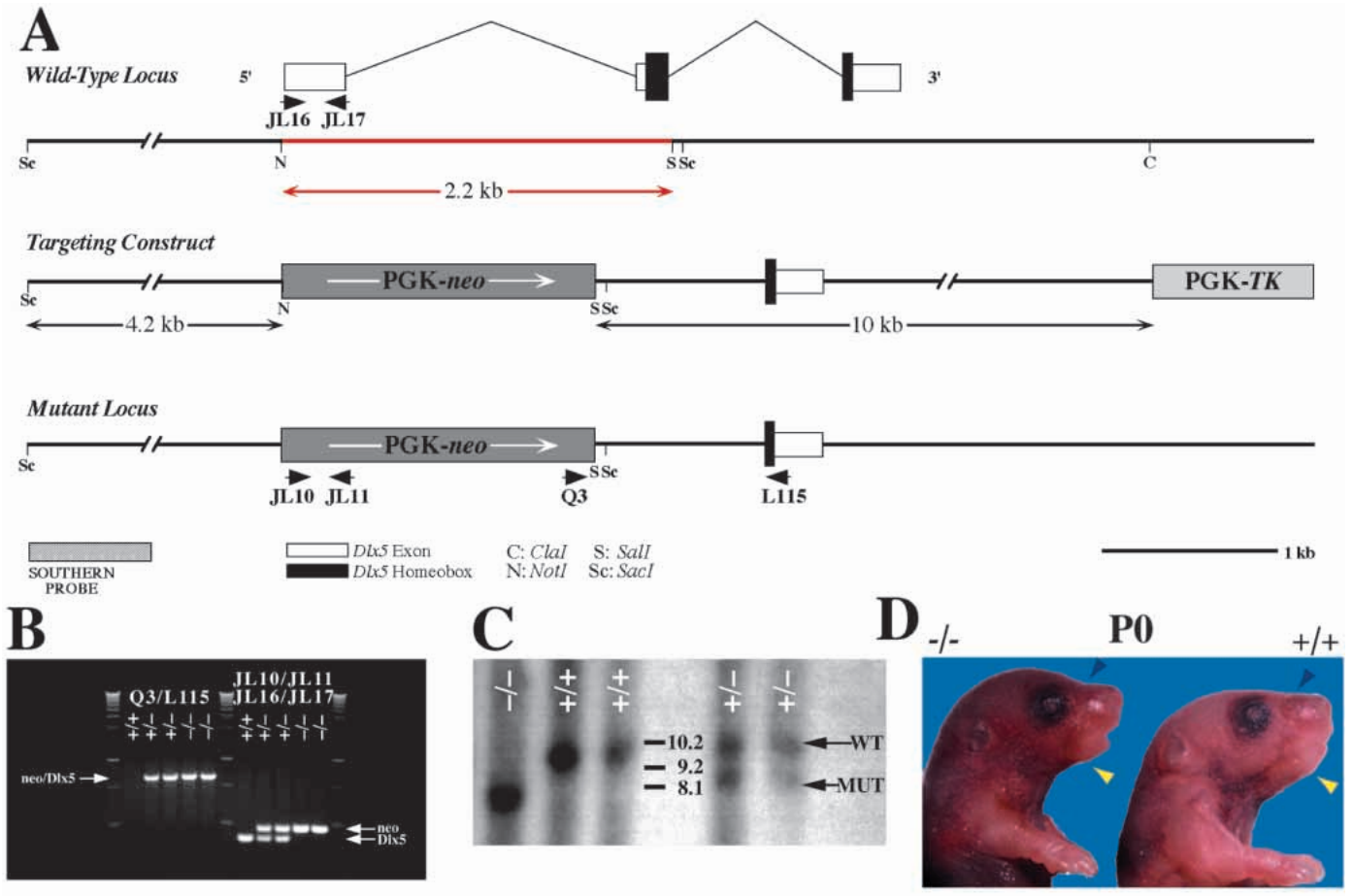

Fig. 2. Diagrams of the structure of the *Dlx5* wild-type gene, targeting construct and mutant locus (A), PCR genotyping (B), Southern genotyping (C) and external anatomy of the upper (anterior) bodies of mutant and wild-type P0 pups (D). (A) Top line: diagram of the genomic organization of *Dlx5* on mouse chromosome 6 and the location of one pair of PCR primers used for genotyping (JL16-JL17). Open boxes represent exons; black boxes represent the homeobox in exons two and three; the red line represents the deleted 2.2 kb sequence. Middle line: diagram of the targeting construct. The grey boxes represent the PGK-*neo* (dark) and PGK-*TK* (light) cassettes. Bottom line: diagram of the mutant locus. The location of other PCR primers used for genotyping (JL10-JL11 and Q3-L115) are indicated beneath. (B) Photograph of an agarose gel showing the DNA products from PCR reactions involving (1) primers Q3/L115 (*Dlx5*/neo; ~1200 bp), and (2) primers JL10/JL11 (PGK-*neo*; 459 bp) and JL16/JL17 (*Dlx5*; 368 bp) double PCR. Size markers are flanking. (C) Southern analysis of *Sac*I-digested genomic DNA. The wild-type fragment is 9.6 kb and the mutant fragment is 7.9 kb. (D) P0 mutants (–/–) are distinguishable from wild-type (+/+) pups by the morphology of their noses (blue arrowheads) and mandibles (yellow arrowheads). The lower (posterior) regions of their bodies appear normal. Abbreviations: C, *Cla*I; N, *Not*I; S, *Sal*I; Sc, *Sac*I.

(placodes) in the surface ectoderm focally regulate skeletal and dental development within the underlying mesenchyme. For example, extirpation and transplantation studies suggest that the olfactory and otic placodes regulate the development of the cartilaginous nasal and otic capsules, respectively (Corsin, 1971; Frenz and Van de Water, 1991; Webb and Noden, 1993).

Craniofacial ectomesenchyme appears to be endowed with some positional information. Coherent streams of CNC migrate along distinct pathways from the dorsal margins of the posterior diencephalon, mesencephalon and metencephalon to contribute skeletogenic mesenchyme to the rostral cranium and distinct domains of the branchial arches (Tosney, 1982; Serbedzija et al., 1992; Osumi-Yamashita et al., 1994, 1997; Imai et al., 1996; Köntges and Lumsden, 1996). Both transplantation and genetic studies provide evidence that A/P specification processes within the neural plate and brain have important roles in imparting regional identity to the CNC, which in turn controls its later development (Noden, 1983, 1991; Gendron-Maguire et al., 1993; Rijli et al., 1993, 1998; Matsuo et al., 1995; Kuratani et al., 1997). While certain genes (e.g. *Otx2* and the *Hox* genes) may regulate A/P specification of the CNC, other homeobox transcription factors appear to influence craniofacial morphology through regulation of CNC development along other axes (e.g. *Dlx*, *Gsc*, *Msx*, *Pax* and *Prx* genes).

Members of the *Dlx* gene family are expressed in both craniofacial ectoderm and CNC (Dollé et al., 1992; Bulfone et al., 1993; Akimenko et al., 1994; Robinson and Mahon, 1994; Simeone et al., 1994; Ellies et al., 1997; Qiu et al., 1997; Yang et al., 1998). Analysis of the expression and function of the murine *Dlx* gene family suggests that these genes might specify regional fate of the branchial arch ectomesenchyme (Qiu et al., 1997). In the first arch, *Dlx1* and *Dlx2* are expressed in both the maxillary and mandibular components, whereas *Dlx3*, *Dlx5* and *Dlx6* are expressed only in the mandibular. In the second (hyoid) arch, *Dlx1* and *Dlx2* are expressed throughout the

proximodistal axis, while *Dlx3*, *Dlx5* and *Dlx6* are only expressed in more distal regions. Mice lacking *Dlx1* or *Dlx2* have deletions and/or morphological transformations of maxillary and proximal hyoid arch-derived structures; the skeleton of the mandibular and distal hyoid arch, however, appears to be normal (Qiu et al., 1995, 1997). The finding that *Dlx1* and *Dlx2* expression is not required in the mandibular and distal hyoid arches suggests that other *Dlx* genes compensate in these regions (Qiu et al., 1997).

Herein, we provide evidence that *Dlx5* regulates craniofacial development both through its expression in ectodermal placodes and ectomesenchyme. *Dlx5* is expressed both in the olfactory and otic placodes, their derived epithelia and the CNC of the mandibular arch (Simeone et al., 1994; Qiu et al., 1997; Yang et al., 1998). Mice homozygous for *Dlx5* mutant alleles die shortly after birth, some with exencephaly. Non-exencephalic mutant mice have hypomineralized calvaria, and all mutants have regional defects in their nasal and otic capsules and proximal mandibles. We hypothesize that *Dlx5* acts in concert with other *Dlx* genes in patterning the ectomesenchyme of the branchial arches. A number of the observed malformations may be due to decreased expression of the *goosecoid* (*Gsc*) homeobox gene.

MATERIALS AND METHODS

Generation of *Dlx5* mutant mice

Genomic DNA encoding the *Dlx5* gene was isolated by screening a genomic library (from Anton Berns, Amsterdam) made from liver DNA isolated from strain 129-J mice using a *Dlx5* cDNA (Liu et al., 1997) as a probe. The targeting construct was made using the pBS KS$^-$ cloning vector. The organization of the targeting vector is shown in Fig. 2. Briefly, a 4.2 kb *Not*I *Dlx5* genomic fragment (upstream of the *Not*I site in the first exon of *Dlx5*) was ligated 5′ to the positive selection gene cassette (PGK-*neo*; Tybulewicz et al., 1991). A 10 kb *Cla*I-*Hin*cII *Dlx5* genomic fragment was subcloned 3′ of the PGK-*neo* cassette. Finally, a negative selection gene cassette (PGK-*thymidine kinase* (PGK-TK); Johnson et al., 1989) was inserted 3′ to this 10 kb fragment. The *Dlx5* targeting construct contains a 2.2 kb deletion of exons 1 and 2, which spans the entire N terminus of the protein and includes the 5′ end of the homeobox.

The targeting vector was introduced into the JM-1 line of ES cells (Qiu et al., 1995). Genotyping of the clones was performed by digesting the genomic DNA with *Sac*I, separation on a 0.5% agarose gel, transfer to a Duralon UV membrane (Stratagene) and high stringency Southern analysis (Sambrook et al., 1989). The Southern probe was a 1.5 kb *Nhe*I-*Kpn*I fragment from *Dlx5* genomic clone 6N6#1 (schematized in Fig. 2). The wild-type fragment appears as a 9.6 kb band and the mutant as a 7.9 kb band. PCR conditions, using Taq polymerase (Qiagen), are as follows: 97°C, 2 minutes (1 cycle); 97°C, 1 minute, 55°C, 1 minute, 72°C, 1 minute (30 cycles); 72°C, 5 minutes (1 cycle). Primers JL16 (CAG TAG AAG AAC AGC CAC) and JL17 (ACT CGG GAC GCG GTT GTA) were used to generate a 368 bp PCR fragment to determine the presence of the first exon of *Dlx5*. Primers JL10 (CAA GAT GGA TTG CAC GCA G) and JL11 (CAT CCT GAT CGA CAA GAC) were used to generate a 459 bp PCR fragment to determine the presence of the PGK-*neo* cassette. Primers Q3 (TCG CAG CGC ATC GCC TTC TAT CGC) and L115 (CCC GTT TTT CAT GAT CTT C) were used to generate an ~1.2 kb PCR fragment to verify the presence of the PGK-*neo* cassette inserted into the *Dlx5* locus.

The ES cell lines containing mutations in one of the *Dlx5* alleles were karyotyped, injected into blastocysts isolated from C57BL/6J mice and then re-implanted into the uteri of pseudopregnant CD-1 mice (Joyner, 1993). Male chimeras were then mated with C57BL/6J females. Germline transmission was assessed by scoring the F_1 offspring for the agouti phenotype and then verified by Southern and PCR analysis (see above). *Dlx5* homozygotes from two independent cell lines (#s 19, 26) had defects in the same structures.

Anatomical analyses

Animals were fixed in 4% paraformaldehyde (PFA) in phosphate-buffered saline (PBS), embedded in paraffin (E10.5-E16.5) or OCT (P0), and then cut in 8 to 20 μm thick serial sections. Sections were then stained with either Gimori trichrome (E10.5-E16.5) or Cresyl violet (P0). Differential staining of cartilage and bone was achieved through the use of Alcian blue and Alizarin red S (McLeod, 1980).

Scanning electron microscopy

Embryos were taken from timed pregnancies and fixed at 4°C overnight in 4% PFA in PBS. The embryos were then rinsed three times in PBS and dehydrated in an increasing series of EtOH. They were critically point dried, sputter coated with gold-palladium and photographed in a JEOL 840 scanning electron microscope.

RNA in situ hybridization

In situ hybridization was performed as described by Shimamura et al. (1995) and Qiu et al. (1997). The *Dlx5* probe was produced from a 1 kb cDNA containing the homeobox and 3′sequence (Qiu et al., 1997). The *Gsc* probe was obtained from Dr E. M. De Robertis. For the *Gsc* in situs, hemisected mutant and wild-type embryos were assayed in the same tube. The contralateral hemisections were hybridized with positive control probes (e.g. *Msx2*).

Whole-mount immunohistochemistry

Neurofilaments were detected with a 4:1 dilution of the 2H3 155 kDa neurofilament antibody (Developmental Studies Hybridoma Bank, University of Iowa) using whole-mount immunohistochemistry, utilizing the Vector ABC kit and following the general procedures described by Qiu et al. (1995).

RESULTS

Expression of *Dlx5*

Dlx5 mRNA is detected in distinct ectodermal tissues (Akimenko et al., 1994; Simeone et al., 1994; Zhao et al., 1994; Liu et al., 1997; Yang et al., 1998). At E8.25 (2- to 4-somite stage), *Dlx5* transcripts are found in the neural ridge at all axial levels (Fig. 1). The anterior neural ridge (ANR), which expresses high levels of *Dlx5* (Fig. 1A), contains the primordia of the forebrain, olfactory placodes, Rathke's pouch and midfacial ectoderm (Couly and Le Douarin, 1985, 1987; Eagleson et al., 1995; Rubenstein et al., 1998), and may be an organizing center for forebrain and facial development (Shimamura and Rubenstein, 1997). During later stages, *Dlx5* expression is maintained in the olfactory placode (Fig. 1F), invaginating olfactory pit (Fig. 1I) and forebrain (Fig. 1J; Simeone et al., 1994; Liu et al., 1997; Yang et al., 1998). The neural ridge, which produces the neural crest and forms the dorsal midline (roof plate), continues to express *Dlx5* at least through E9.0 (Fig. 1C,F,H). *Dlx5* transcripts are detected in the otic placode and its derivative, the otic vesicle (OV; Fig. 1C,F,G). Its expression is highest in the dorsal regions that are the anlagen of the endolymphatic duct (ED) and the vestibular apparatus (Sher, 1971; Van de Water, 1984). *Dlx5* is also expressed in postmigratory CNC cells in the branchial arches

(mandibular first arch and distal parts of the caudal arches) (Fig. 1C,F,G,I; Simeone et al., 1994; Zhao et al., 1994; Qiu et al., 1997). *Dlx5* expression can be seen at later stages (Fig. 1J) during organogenesis of the skeleton (Simeone et al., 1994; Zhao et al., 1994; Chen et al., 1996).

Generating *Dlx5* mutant mice

We used the JM-1 line (strain 129) embryonic stem (ES) cells (Qiu et al., 1995) for targeted mutagenesis of murine *Dlx5*. The targeting vector was designed to make an approximately 2.2 kb deletion to eliminate the N terminus of *Dlx5*, including 43 amino acids of the homeodomain (Fig. 2). Four ES clones harboring one *Dlx5* mutant allele were identified. We made chimeric mice from two of these clones. The chimeras were out-bred with C57BL/6J mice to generate heterozygotes. Inbreeding of these mice produced exencephalic newborns (7/259, or ~3%) which were heterozygous for the mutant *Dlx5* allele. The frequency of exencephalic heterozygotes has greatly diminished with further outbreeding to C57BL/6J mice. Other than exencephaly, no other phenotypes have been noted in heterozygotes – except that these mice do not breed readily. Inbreeding of heterozygotes was used to generate *Dlx5* homozygous mutant animals. Of 29 litters tested, a genotypic ratio of 31%:51%:18% (81 +/+:132 +/–:46 –/–) was determined. Newborn *Dlx5* mutant mice are slightly smaller than their wild-type littermates (Fig. 2D) and lack milk in their stomachs. All *Dlx5* homozygous mutants die shortly after birth.

Dlx5 homozygote mutant newborns have cranial defects

Several external craniofacial defects are apparent in the *Dlx5* homozygous mutant newborns, including decreased nasal capsular breadth, micrognathia and malformed auditory pinnae (Fig. 2D). Exencephaly was evident in 28% of the animals (Fig. 3; Table 1). Scanning electron microscopic analysis of *Dlx5* mutant embryos suggests that the neural tube closure defect is centered in the midbrain but can include the forebrain and hindbrain in severe cases (Fig. 3A-D). The calottes (calvarial roofs; White and Folkens, 1991) of non-exencephalic *Dlx5* mutants have small, hypomineralized parietal and interparietal bones (Fig. 3F). The supraoccipital, though reduced in size, is less affected. The occipital arch cartilages are thicker and expanded rostrocaudally. Increased amounts of secondary cartilage form in the sagittal and lambdoidal sutures (data not shown). The remainder of the calotte (e.g. frontals) appears to have normal mineralization as assayed by Alizarin Red S staining.

All cranial bones have at least subtle dysmorphologies, which we suggest are due to epigenetic factors (e.g. biomechanical influences) and/or altered skeletal differentiation. Because *Dlx5* is expressed in developing skeletal elements (Fig. 1J; Simeone et al., 1994; Zhao et al., 1994; Ferrari et al., 1995; Chen et al., 1996), these malformations may result from a lack of *Dlx5* functioning during skeletogenesis. For example, the primary and secondary palates exhibit variable degrees of clefting and components of the cranial sidewall (e.g. the alisphenoid and squamosal) have slight morphologic alterations (data not shown). Although *Dlx5* is expressed in the post-cranial axial and appendicular skeleton (Simeone et al., 1994; Zhao et al., 1994; Ferarri et al., 1995; Chen et al., 1996), we detected few abnormalities in these structures. The angle of the ribs, for example, appeared sinusoidal in 27% of cases (data not shown). *Dlx5* mutant animals – with or without exencephaly – exhibit the same set of additional craniofacial abnormalities (see below and Table 1).

Table 1. Phenotypic penetrance of defects in *Dlx-5*$^{-/-}$ skulls*

Calotte		
Hypomineralized	100%	(18/18)‡
Exencephalic	28%	(6/24)
Otic capsule		
Pars Canalicularis	100%	(23/23)
Pars Cochlearis	100%	(21/21)
Tegmen Tympani	100%	(18/18)
Nasal capsule		
Paries Nasi/Turbinates	100%	(30/30)
Asymmetry	85%	(25/30)
>Hypoplasia on R	88%	(22/25)
TP-NS rod-like	30%	(9/29)
Brachial arch		
Mandibular	100%	(31/31)
Os Paradoxicum	100%	(31/31)
Palate		
Clefting	88%	(22/25)
Parapalatines	88%	(22/25)

*Based upon evaluation of bone and cartilage preparations.
‡(x,y) where x/y represents a total of P0 and E15.5 animals examined for which scoring was possible.

Dlx5 mutants have defects in olfactory placode and frontonasal prominence derivatives

In *Dlx5* mutant newborns (P0), chondrocranial and dermatocranial defects are observed in and around the nasal capsule and mesethmoid (Fig. 4). In the most severe cases, there is symmetric, near aplasia of the capsule and mesethmoid (Fig. 4AIII,E). A midline cartilaginous rod-like extension of the rostral trabecular cartilage forms but fails to develop a dorsoventrally expanded nasal septum. Small, cartilaginous spicules are the only remnants of the side walls of the capsule (paries nasi, prominentia lateralis and associated turbinates). The posterior capsule and mesethmoid are reduced to thin, planar orbitonasal laminae (Fig. 4AIII,E): in these cases, there is no evidence for the development of a nasal epithelium, nor of a true tectum or solum [including the paraseptal cartilages and associated vomeronasal organ (VNO)] of the nasal capsule.

In cases of intermediate severity (the majority of cases observed), a pronounced asymmetry, with the right side being more hypoplastic, is seen (Fig. 4AII,D; Table 1). The trabecular plate-nasal septum, which is compressed dorsoventrally, deviates to the right to occupy the position of the right cribriform plate and posterior nasal capsular wall (Fig. 4AII). No foramina cribrosa are seen on the right and very few on the left. The tectum nasi, solum and paries nasi prominences and associated turbinates (e.g. frontoturbinates and ethmoturbinates) are hypoplastic. In these less severe cases, rudimentary branches of the nasal epithelium are present (Fig. 4D), as are hypoplastic rostral turbinate cartilages (data not shown). Cartilages in the floor of the nasal capsule (e.g. lamina transversus anterior and paraseptal cartilages) are hypoplastic and sometimes associated with a rudimentary VNO (data not shown). The dermal bones

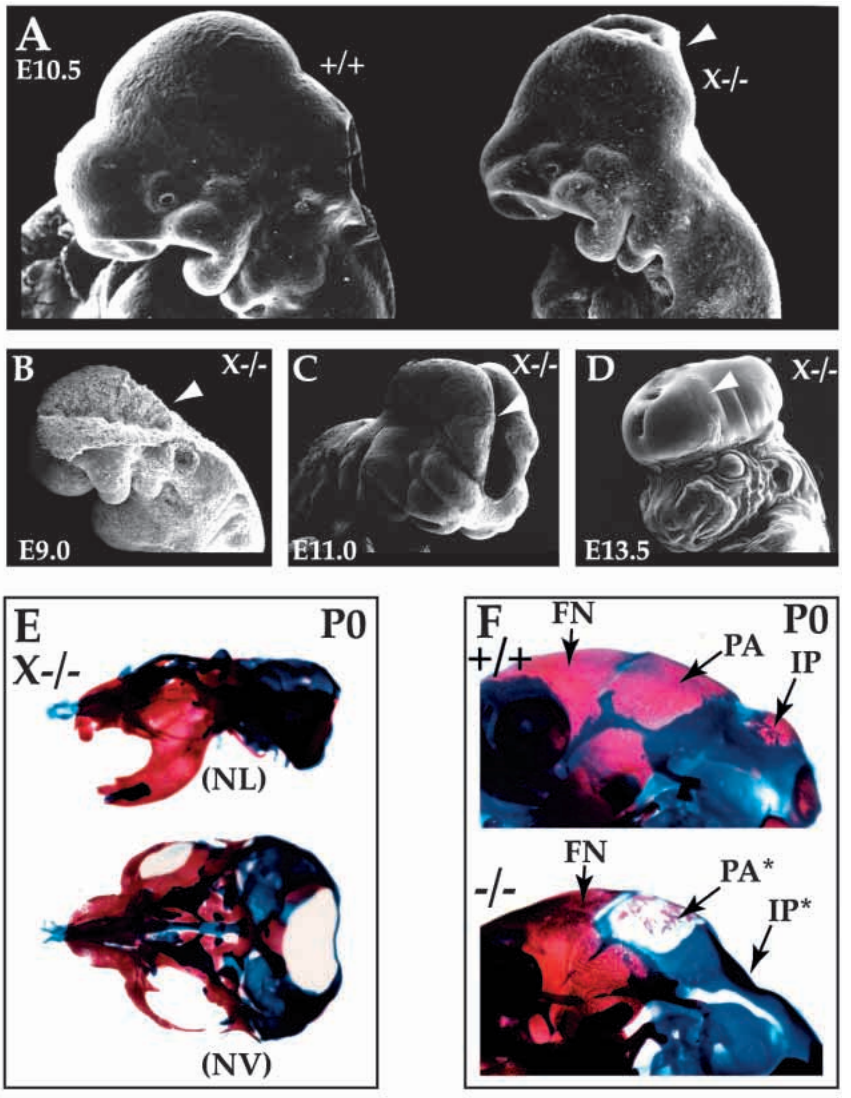

Fig. 3. *Dlx5* mutants exhibit exencephaly (X) and hypomineralization within the calotte.
(A-D) Scanning electron micrographs of the exencephalic phenotype. (A) E10.5 wild-type (+/+) and exencephalic mutant (X –/–). The white arrowhead indicates the open neural tube. (B-D) Appearance of the exencephalic phenotype, highlighted by white arrowheads, at E9.0 (B), E11.0 (C) and E13.5 (D). The defect is generally centered around the midbrain and can extend rostrally and caudally. (E) Differential staining of bone (red) and cartilage (blue) of an exencephalic (X –/–) P0 mutant as viewed laterally (norma lateralis, NL) and dorsally (norma verticalis, NV). The nasal capsules, otic capsules and branchial arches of the exencephalic and non-exencephalic mutants have the same dysmorphic phenotypes (see Figs 4-6; Table 1). (F) Comparison of the dorsolateral skull of wild-type (+/+) and mutant (–/–) P0 mice highlights the hypomineralization of the parietals (PA*) and interparietals (IP*) of the mutant.

that encase the nasal capsule (e.g. nasals, premaxillae, maxillae, vomers and lacrimals) are dysmorphic and small.

In light of *Dlx5* expression in the ANR and its olfactory derivatives (Fig. 1), we searched for early defects in this region and found evidence of hypoplasia of the frontonasal prominences (FP) at E10.5 (data not shown). These defects are usually asymmetric, with the right side being more affected than the left. As emphasized by scanning electron microscopy at E12.5, the lateral frontonasal prominence typically appears very small (Fig. 4B).

Dlx5 is required for the development of inner ear vestibular components and associated otic capsule

Dlx5 transcripts are detected during otic placodogenesis, otic pit invagination and the development of the OV (Fig. 1). The OV gives rise to specialized epithelial tissues of the vestibular and cochlear apparati of the inner ear (Sher, 1971; Van de Water, 1984; Fritzsch et al., 1998; Torres and Giraldez, 1998). Mesodermal and ectomesenchymal cells surrounding the inner ear form the chondrocranial otic capsule (Van de Water, 1984; Couly et al., 1993). The otic capsule has two major regions: (1) the pars canalicularis (PCa), which houses the vestibular system (semicircular canals (SCC) and utricle) and the endolymphatic duct, and (2) the pars cochlearis (PCo), which houses the auditory apparatus. The PCa is malformed and hypoplastic in the *Dlx5* mutants as the anterior and posterior SCC do not form (Fig. 5BIII, V). The lateral SCC has a complete, but shortened, cartilaginous canal (Fig. 5BIV). The maculae and papillae are present, but the ED does not develop (Fig. 5BI). The perilymphatic duct, however, is roughly the size of the utricle. The PCo is smaller: the cochlea completes roughly only one coil (compared to the usual one and a half; Sher, 1971) and the fenestra cochlea is anomalous in size and orientation (Figs 5BV, 6D). Spiral laminae are abnormal: a cartilaginous shelf seems to separate the cochlea from the scala vestibulae (data not shown).

The otic capsules, middle ear ossicles and associated soft tissues have several additional dysmorphic features. The epitympanic recess is expanded, and the tegmen tympani (TT) is hypertrophied (Fig. 5BV) and extends rostrally as an enlarged cartilaginous lamina. The TT maintains a prolonged synovial contact with the malleus and incus, and it shares origins for the tensor tympani with a novel structure, the os paradoxicum (OP; discussed below), and the gonial (data not

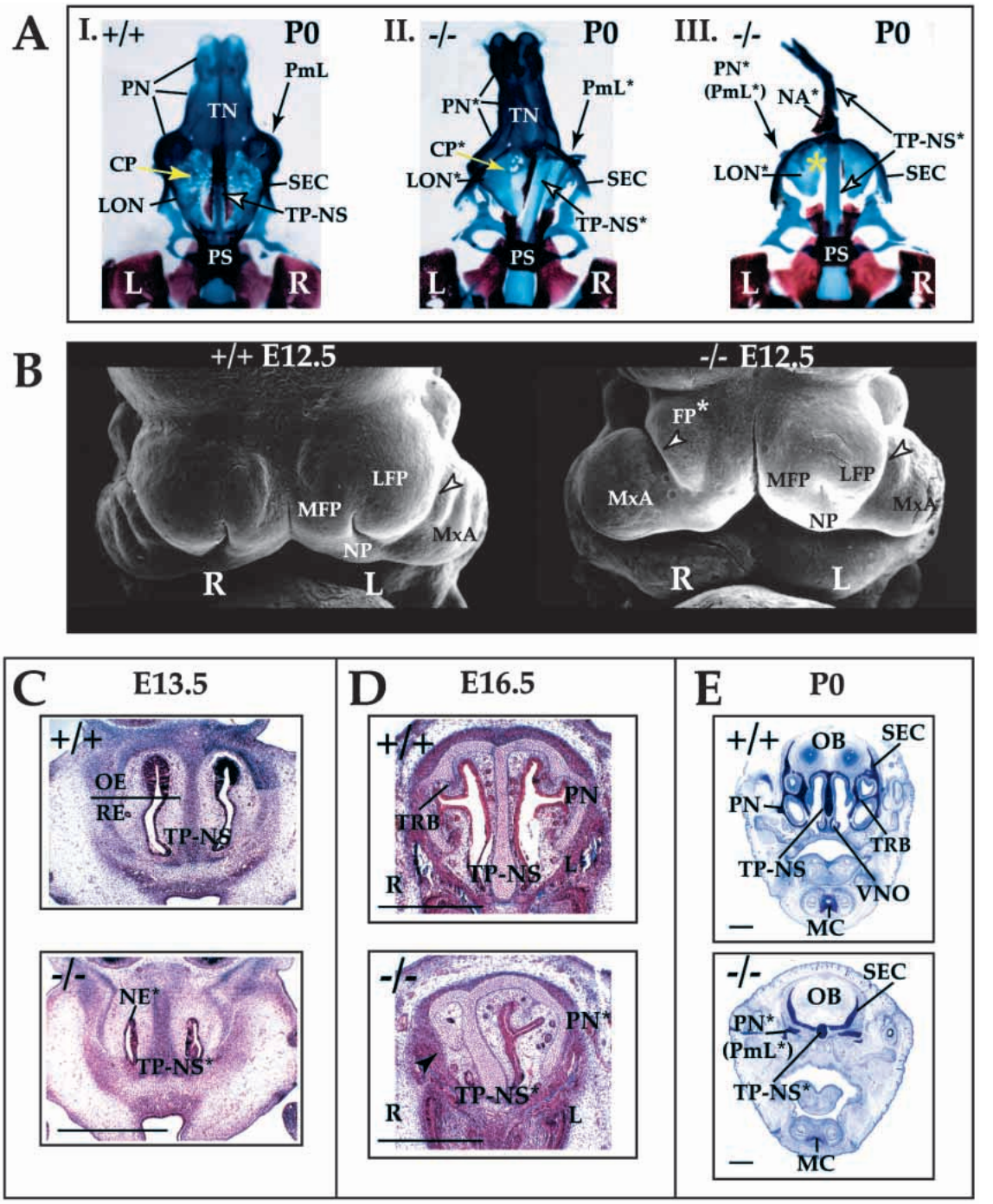

Fig. 4. *Dlx5* mutants exhibit a range of defects in the frontonasal prominences and associated structures, including a prominent asymmetry of the nasal capsule. (A) Differential staining of bone (red) and cartilage (blue) of a wild-type (I), a mutant of intermediate severity with nasal asymmetry (II), and a severely affected mutant (III). Asterisks indicate highly dysmorphic structures. In AII, the trabecular plate-nasal septum (TP-NS*) deviates to the right, occupying the space of the posterior nasal capsule, right cribriform plate (CP) and mesethmoid. The mutant in AIII exemplifies the most severe phenotypic type that we observe: it has a trabecular rod (TP-NS*) with near agenesis of the nasal capsule and cavity (LON*, PN*). The deviation seen in the rostral tip of the TP-NS* is artifactual. The mutant nasal bone (NA*) has not been removed to maintain connection within the TP-NS*. The yellow asterisk denotes the relative position of the left side of the mesethmoid. (B) Scanning electron micrographs of E12.5 wild-type and mutant embryos show the severe hypoplasia of the right frontonasal prominences (FP*); the lateral frontonasal prominence (LFP) appears to be more severely affected than the medial frontonasal prominence (MFP). Arrowheads demarcate the nasolacrimal grooves, which develop lateral to the prominences. (C-E) Coronal sections through the nasal capsules of E13.5, E16.5 and P0 wild-type and mutant animals: the mutant in C has mild hypoplasia; the mutant in D has severe hypoplasia of the right side (as in AII); the mutant in E has severe bilateral hypoplasia (as in AIII). (C) Wild-type and *Dlx5* mutant E13.5 embryos. While both embryos developed nasal pits, the nasal cavity of the mutant is rudimentary. Development of distinct olfactory (OE) and respiratory (RE) epithelia, evident in the wild-type embryo, is not clear in the mutant. Failure to form a VNO and supporting paranasal cartilages is frequently observed (not shown). (D) Wild-type and *Dlx5* mutant E16.5 animals. The mutant has a pronounced asymmetry of the nasal capsule with a nearly complete loss of the right nasal apparatus (arrowhead). (E) Wild-type and severely affected *Dlx5* mutant P0 pups. Note also the lack of a VNO. Abbreviations: CP, cribriform plate; FP, frontonasal prominences; LFP, lateral frontonasal prominence; LON, lamina orbitonasalis; MC, Meckel's cartilage; MFP, medial frontonasal prominence; MxA, maxillary arch; NA, nasal bone; NE, nasal epithelium; NP, nasal pit; OB, olfactory bulb; OE, olfactory epithelium; PmL, prominentia lateralis; PN, paries nasi; PS, presphenoid; RE, respiratory epithelium; SEC, sphenethmoidal commissure; TN, tectum nasi; TP-NS, trabecular plate-nasal septum; TRB, turbinate; VNO, vomeronasal organ.

shown). The TT is also linked to the alicochlear commissure via an anomalous fibrous tract, and the belly of the stylopharyngeus lies ventral and superficial to the ear drum, most likely precluding functionality (data not shown). The external acoustic meatus is shortened and the tubal cartilage develops in nodules (data not shown).

Dlx5 is required for proper development of branchial arch derivatives

In *Dlx5* mutants, the chondrocranial element of the mandibular arch, Meckel's cartilage (MC), is shortened (Fig. 6D,F). As early as E13.5, the proximal shaft of MC is extremely dysmorphic; this is clearly seen at E15.5 (Fig. 6D,F). The orientation of MC deviates twice (n=5/5 at E15.5). Initially projecting caudolaterally, MC sharply deviates laterad at a point near its proximocaudal end adjacent to the proximal end of the dentary (DNT; Fig. 6D,F). It then abruptly reorients caudomedially for a short distance whereupon it splits: a medial branch forms an ectopic strut towards the pterygoid and basisphenoid; the other branch continues caudolaterally into the malleus. By P0, ectopic intramembranous bones invest the cartilaginous strut (Fig. 6H). We have named this novel ectopic strut and associated ossification, the os paradoxicum (OP; Fig. 6D,F,H). The OP may invest, or form a synovial joint with, the pterygoids. It also forms a synovial joint with the misshapen gonial and sutures with the anterior crus of the tympanic. The malleus has a smaller than normal processus brevis and is caudally extended and thickened at the level of the manubrium. The tympanic is slightly smaller and thicker (data not shown).

A short and dysmorphic DNT develops around the abnormal MC (Fig. 6D,F,G). The proximal lamina of the coronoid is absent, and the condylar and angular processes are shortened, misshapen and juxtaposed (Fig. 6G). Often an ectopic, proximodistally oriented cartilaginous and osseous spicule develops along the buccal surface of the condylar process (data not shown). This appears to run toward (and form a synovial joint with) the hypotrophic jugal bone – itself reoriented toward the condyle at the expense of its articulation with the zygomatic process of the squamosal (not shown). Buccally, the temporalis muscles are attached to what might represent a displaced, vestigial distal coronoid process (minus the proximal extension), which runs parallel to the mandibular body, lateral to the molar teeth (not shown). Extensive chondroid bone develops along the incisive alveolar bone at the tips of the dentary; the incisivium itself is broader and shorter than normal. The dental canal/lingula is reflected lingually (medially) at the angular end (with the mylohyoid line extended caudad). The molar alveolae are shorter, broader and deeper. The alveolar openings are constricted distally and broadened proximally. The buccal molar walls are less robust and ventrally reflected.

Not surprisingly, this region supports anomalous muscle development. The OP acts as an origin for the medial pterygoid (which is hypertrophied) and tensor palati muscles; normally, these muscles originate from fibrous connective tissue in regions where the alisphenoid and the tegmen tympani of the otic capsule ossify (data not shown). The medial pterygoid insertion groove is occluded by a broad origin for an abnormal mylohyoid. Moreover, the rostral limit of the genioglossus and geniohyoid muscles are displaced caudad along the mylohyoid line, and there are numerous, ectopic connections to the hard tissue (data not shown). Dorsocaudal to the mylohyoid, anomalous fascicles of the genioglossus muscle run from the mylohyoid, lingula, OP and gonial into the tongue. The buccinator muscles attach mandibulae to maxillae such that there is no slack in the buccal pouch (data not shown).

There is variable palatal clefting exemplified by defects in palatine and maxillary morphology (data not shown). Ectopic membrane bones, here referred to as parapalatines (PrP), consistently (88%, Table 1) develop caudal to the palatine shelves and rostral to dysmorphic pterygoids. The pterygoids have an abnormal amount of chondroid bone and secondary cartilage. The right side of the rostral tongue is generally hypertrophied vertically, filling in the right side of the palate and leaving the left side to fill in under the incisors (not shown).

There are additional anomalies of soft-tissue anatomy, often asymmetric, not detailed here, that variably affect the courses of the stapedial artery, the lingual duct and the fascicle pattern of the intrinsic tongue musculature. The larynx, furthermore, is displaced caudally and occupies a position well back from the pterygoids and tympanic cavity (data not shown). The superior cornu (SC) of the thyroid cartilage (TC; derived from the fourth branchial arch, Patten and Carlson, 1988) consistently fail to form (Fig. 6I).

Dlx5 is expressed during dental development (Simeone et al., 1994; Weiss et al., 1994, 1995, 1998). Unlike the *Dlx1/2* mutants, which lack maxillary molars, molar teeth are present in the *Dlx5* mutants (except for the maxillary and mandibular third molars, which are frequently absent in wild-type mice; Grüneberg, 1963). The mandibular and maxillary molars appear to have malformed and poorly mineralized crowns, and both sets of incisors are shortened and misshapen (data not shown).

To assess whether disruption of craniofacial patterning in the *Dlx5* mutant affects the growth of the cranial nerves, we compared the axonal trajectories in wild-type (n=5) and mutant (n=2) embryos at E10.5 using the 2H3 neurofilament antibody (Fig. 6A,B). In the mutant embryos, the trigeminal ganglion is smaller (Fig. 6B), its root appears malformed and it has reduced axonal projections into the surrounding mesenchyme (especially V_2 and V_3). Other axonal defects were found in the processes of the hypoglossal nerve, the autonomic ganglionic chain (AGC) and the dorsal root ganglion (Fig. 6B and data not shown). At later stages, trigeminal nerve axons extend further into the branchial arches, although their orientations are abnormal based upon the morphology of their foramina [e.g. the mental foramen (Fig. 6F)].

Dlx5 regulates the expression of *Gsc*

Because *Gsc* mutants lack turbinates within their nasal capsules, and have altered mandibular branchial arch, ear and mesethmoid morphologies (Rivera-Perez et al., 1995; Yamada et al., 1995, 1997; Belo et al., 1998), we compared the expression of *Gsc* in wild-type (n=2) and *Dlx5* mutant (n=2) embryos. In situ hybridization of hemisected control and mutant embryos at E10.5 revealed a decrease, or loss, of *Gsc* within the mesenchyme of the branchial arches and the frontonasal prominences of the olfactory pits (Fig. 7I).

DISCUSSION

The development of the skull depends upon interactions between epithelial (surface ectoderm, neural tube and

endoderm) and mesenchymal (CNC and mesoderm) tissues (Hall, 1991; Hanken and Hall, 1993; Hanken and Thorogood, 1993; Francis-West et al., 1998). Evidence described herein suggests that *Dlx5* expression is required in specialized epithelial tissues (placodes) for nose and ear development, whereas it is required in the ectomesenchyme of the mandibular arch for development of the proximal mandible. *Dlx5* further appears to exert an influence in the differentiation of particular skeletal elements.

Animals that are heterozygous for the *Dlx5* deletion generally appear indistinguishable from wild-type animals, suggesting that this mutation does not act in a dominant manner. We did, however, observe exencephaly in a fraction of *Dlx5* heterozygous animals (~3%) during early passage of this mutant, implying that rostral neural tube closure is sensitive to *Dlx5* dosage in 129-strain mice and that there are compensatory genes in C57BL/6J-strain mice. The non-Mendelian ratios of heterozygous and homozygous newborns suggests that some animals die in utero. A definitive cause of neonatal death has not been determined.

Role of *Dlx5* in skeletal differentiation

Dlx5 is expressed in condensing, differentiating and developing cartilages, bones and teeth (Fig. 1J; Simeone et al., 1994; Weiss et al., 1994, 1995, 1998; Zhao et al., 1994; Chen et al., 1996; Ferrari et al., 1995; Newberry et al., 1998; Ryoo et al., 1997; Thomas et al., 1997, 1998; Xu et al., 1999), implying that it may have a general role in regulating hard tissue development. Three lines of evidence suggest that the *Dlx* genes play roles in osteogenesis and chondrogenesis. First, *Dlx1, Dlx2, Dlx1/2* and *Dlx5* mutants each have abnormal bone and cartilage morphogenesis in the skull. Second, *Dlx5* is expressed in a stage-specific manner in differentiating osteoblasts in vitro, where it may play a role in regulating *osteocalcin* expression, perhaps through inhibition of the Msx2 protein (Ryoo et al., 1997; Newberry et al., 1998). Third, bone morphogenetic protein 2 (BMP-2) can increase *Dlx5* and *Dlx2* expression in osteoblasts and chondroblasts (S. Harris, personal communication). Moreover, antisense oligonucleotides to *Dlx2* repress the transcription induced by BMP-2 of *pro-alpha1(II) collagen* in chondrocytes (Xu et al., 1999).

Consistent with these observations, most of the cranial bones and the teeth in *Dlx5* mutants are dysmorphic. In addition, there are minor defects in the ribs (data not shown). While we suggest that these morphological changes may be due in part to abnormal skeletal differentiation, it is likely that epigenetic factors contribute to the phenotypic abnormalities. For instance, biomechanical effects resulting from malformations of the capsules, splanchnocranium and associated soft tissues may have contributed to abnormal morphogenesis of other cranial structures. We suggest that the mechanisms underlying these general defects in skeletal morphogenesis are distinct from the mechanisms underlying earlier focal defects in the cartilages of the nasal capsule, otic capsules and the proximal mandibular arch (discussed below).

Dlx5 regulates the development of structures derived from the olfactory and otic sensory placodes

Placodes are thickenings in the primitive ectoderm that give rise to a number of structures, including cranial sensory tissues (Jacobson, 1963, 1966; Verwoerd and van Oostrom, 1979; Webb and Noden, 1993). Some placodes invaginate. For instance, the olfactory placodes involute to give rise to the olfactory neuroepithelium, the VNO and the respiratory epithelium of the nasal cavity, and the otic placodes involute to form the vestibular and auditory sense organs. Other placodes contribute cells to cranial sensory ganglia through a process of delamination (Begbie et al., 1999). The olfactory and otic placodes do both (Webb and Noden, 1993). The requirement of *Dlx5* in the development of both olfactory and otic structures suggests that the induction and histogenesis of these tissues may share similar regulatory mechanisms. Although *Dlx5* is expressed at early stages of olfactory and otic placode formation, it does not appear to be required for their initial specification.

Of the defects observed in the *Dlx5* mutants, only those associated with the nasal capsule showed variable severity and asymmetry (Table 1). 85% of *Dlx5* mutants have asymmetric nasal development, of which nearly 90% have greater hypoplasia on the right. This can be seen as early as E10.5 (data not shown) and, by E12.5, it appears as if a lateral frontonasal prominence (LFP) has not formed (Fig. 4B). While there has been recent success in identifying the molecular bases for left-right asymmetry in several organ systems (Levin and Mercola, 1998; Ramsdell and Yost, 1998), it is not yet clear how these findings explain the asymmetry in the *Dlx5* mutants. *Hesx1* mutants also have asymmetric development of the nasal cavity, but we are unaware whether or not the sidedness of the asymmetry is random (Dattani et al., 1998). There are species, moreover, in which midline FP-derived structures are asymmetrically located (e.g. the blow hole of certain whales; Raven and Gregory, 1933; Klima, 1987), or have asymmetric development of the FP-derived upper incisors (e.g. the narwhal, *Monodon monoceros* L.; Eales, 1950). Hence, the developmental potential for asymmetric development of the FP appears to exist.

The induction and invagination of the otic placode is regulated by interactions with endoderm and hindbrain (Jacobson, 1963, 1966; Fritzsch et al., 1998; Torres and Giraldez, 1998). As with the olfactory epithelium, the otic epithelium has been implicated in regulating chondrogenesis of the adjacent mesenchyme to form the otic capsule (Grobstein and Holtzer, 1955; Van de Water, 1984; Van de Water and Galinovic-Schwartz, 1987; Frenz and Van de Water, 1991; Thorogood, 1993; Legan and Richardson, 1997; Fritzsch et al., 1998). Morphological defects can be seen as early as E10.5 in the otic vesicles of *Dlx5* mutants, in particular, the failure to form the dorsally located endolymphatic duct (Fig. 5B). By E13.5, other dorsal derivatives of the pars canalicularis are not detectable, including the anterior and superior semicircular canals and the cartilaginous capsule surrounding them.

Although there is variable penetrance and asymmetry of the dysmorphic features of the nasal capsule, we hypothesize that the defects in both olfactory and otic capsules stem from primary defects in the placode-derived epithelium: an aberrant epithelium forms, but it cannot support normal chondrogenesis in the underlying mesenchyme. This hypothesis is based upon three observations. First, *Dlx5* is expressed in the ectoderm and not the mesenchyme (until after capsulogenesis has begun; Fig. 1 and Simeone et al., 1994; Zhao et al., 1994; Yang et al., 1998). Second, extirpation experiments suggest that the olfactory pit and otic vesicle induce chondrogenesis in the

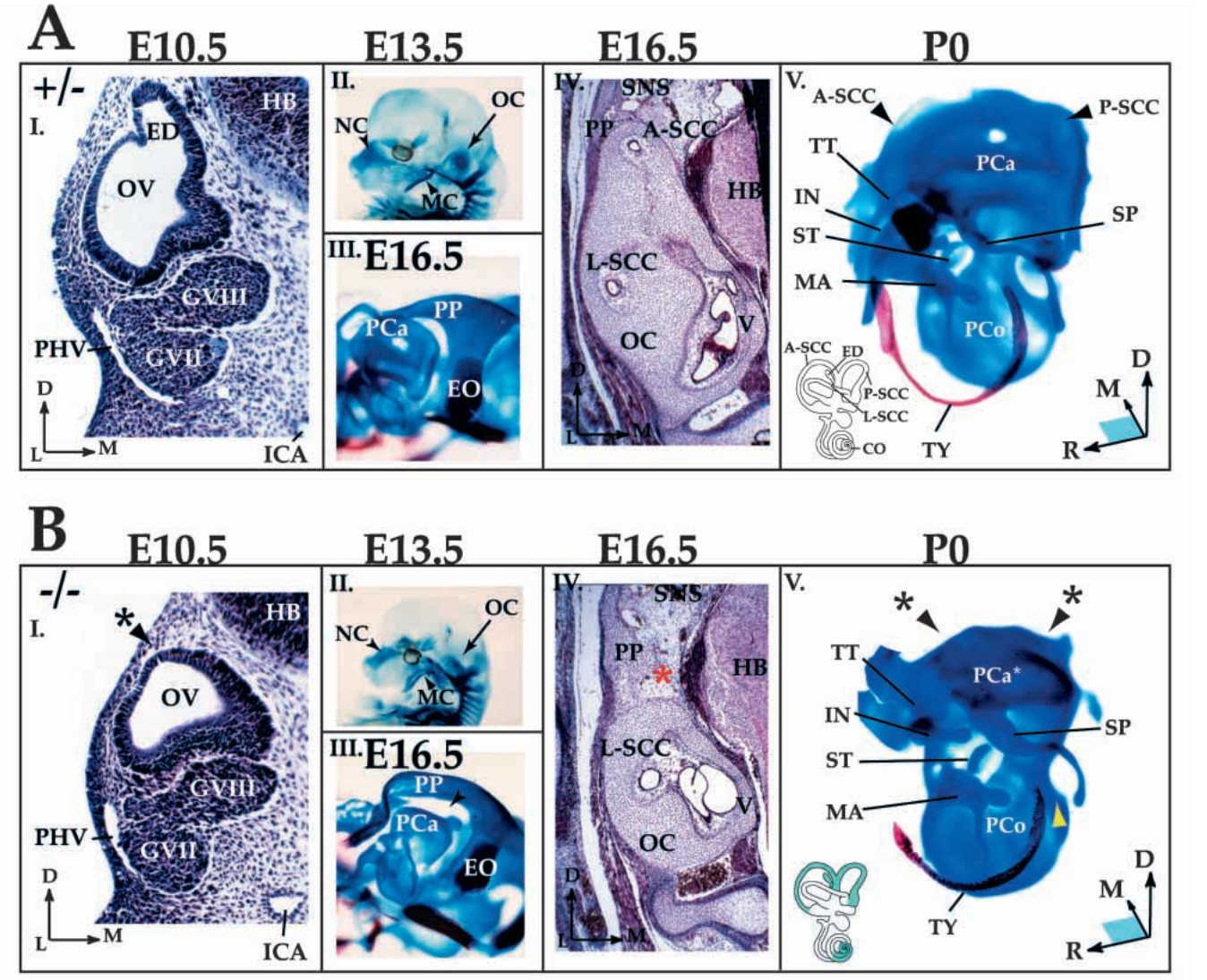

Fig. 5. *Dlx5* is required for proper development of the ear. A: (+/–). B: (–/–). (AI, BI) Sections E10.5 embryos showing early otic vesicular defects in the *Dlx5* mutants. The mutant has failed to form an ED (black asterisk and arrowhead). (AII, BII) Whole-mount cartilage staining reveals defects in the otic capsule (OC) at E13.5. (AIII, BIII) Whole-mount differential bone (red) and cartilage (blue) staining at E16.5 reveals the loss of the anterior and posterior semicircular canals within the pars canalicularis (PCa). The black arrowhead (BIII) points to the resultant expansion of the superior occipito-capsular fissure. (AIV, BIV) Coronal section through the otic capsule at E16.5 shows the loss of the anterior (superior) semicircular canal (A-SCC; red asterisk). The lateral semicircular canal (L-SCC) is malformed, and the perilymphatic spaces have been expanded. (AV, BV) Otic capsules from P0 heterozygous and *Dlx5* mutant pups. The loss of the A-SCC and posterior semicircular canal (P-SCC) has left the pars canalicularis (PCa*) malformed and hypoplastic (black arrowheads marked with asterisks). Moreover, the tegmen tympani (TT) is hypertrophic. The yellow arrowhead indicates the anomalous size and orientation of the fenestra cochlea. The stapes, styloid process and incus are all present. The inset diagrams the components of the inner ear: those parts in green (BV) represent the regions most affected in the mutants.

mesenchyme that forms the surrounding capsules (Corsin, 1971; Frenz and Van de Water, 1991; Webb and Noden, 1993). Third, loss of *Dlx5* in the olfactory epithelium results in a loss of *Gsc* expression in the surrounding mesenchyme (Fig. 7I). Normally at E10.5, *Gsc* is expressed in the mesenchyme of the frontonasal prominences and distal first and second arches (Gaunt et al., 1993). Homozygous mutant *Gsc* animals have defects of the nasal capsule, mesethmoid, mandibular arch derivatives, tongue and ribs (Yamada et al., 1995, 1997; Rivera-Perez et al., 1995; Belo et al., 1998; schematically depicted in Fig. 7J). A number of the defects seen in the *Gsc* null mutants may be considered phenotypic subsets of those observed in *Dlx5* mutants. For example, in both the *Dlx5* and *Gsc* mutants, the nasal turbinates are hypoplastic, the nasal septum fails to extend to the palate (i.e. is shortened dorsoventrally) and the posterior nasal capsule and mesethmoid (e.g. lamina orbitonasalis and cribriform plate) are hypoplastic (Fig. 7J). We suggest, therefore, that *Dlx5* regulates epithelial factors that govern chondrogenesis of the adjacent mesenchyme.

Dlx genes regulate regional morphogenesis of the branchial arches

The *Dlx* genes operate in concert to control histogenesis in the forebrain (Anderson et al., 1997a,b). We have suggested

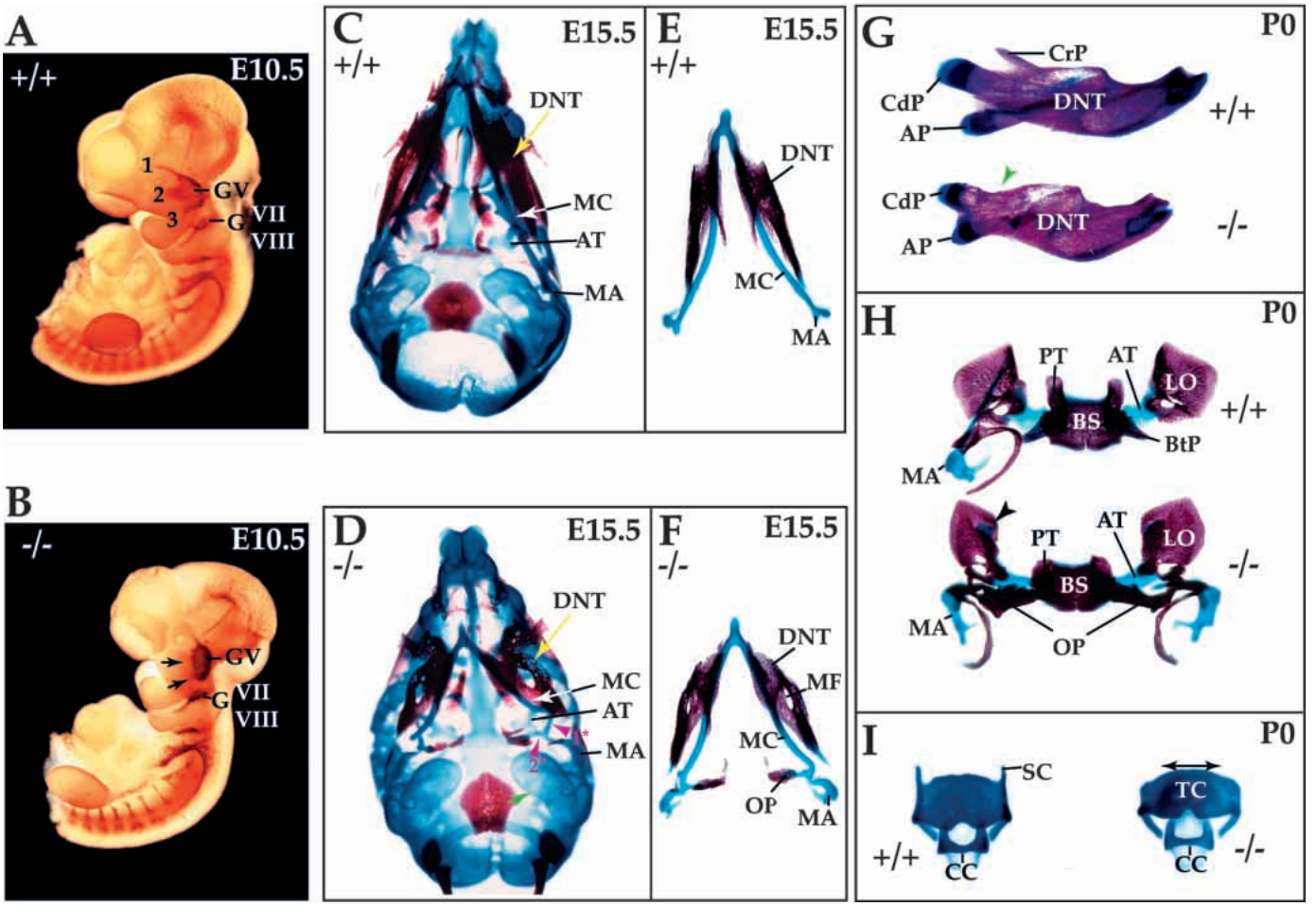

Fig. 6. *Dlx5* is required for the development of the branchial arches and associated structures. (A,B) Whole-mount immunohistochemistry using the 2H3 neurofilament antibody on E10.5 wild-type (A) and *Dlx5* mutant (B) embryos reveals decreased axonal extensions from the trigeminal ganglion (GV; black arrows). (C-F) Differential staining of bone (red) and cartilage (blue) in E15.5 wild-type (C,E) and mutant (D,F) fetuses demonstrates a reorientation of the proximal end of Meckel's cartilage (MC). (C,D) Normally, MC follows a relatively smooth curve from its rostral process (at the symphysis mentalis) to the malleus (MA). In the mutant, MC deviates laterally, and then medially (purple arrowhead 1*) to a bifurcation: one process extends laterally to the MA; the other process projects medially toward the basal plate midline (purple arrowhead 2*). This process forms the cartilaginous core of the os paradoxicum (OP). The green arrowhead highlights anomalies of the cochlea. (E,F) Dissected mandibular arch derivatives (MA, MC, OP and DNT) highlight the deviations of MC and the development of the OP. Note the dorsolaterally oriented mental foramina (MF) in the mutant. (G) Numerous abnormalities are apparent in the development of the DNT at P0. These include: micrognathia, shortening and juxtaposition of the condylar (CdP) and angular (AP) processes, and absence of the proximal lamina of the coronoid (CrP) process (green arrowhead). (H) Dissection, at P0, of the OP and comparison with normal regional anatomy. The basisphenoid (BS), ala temporalis (AT), and basitrabecular process (BtP) develop in the *Dlx5* mutants: the OP forms in a ventral, but parallel plane to these. The OP obscures viewing the BtP in the mutant. The OP forms an ossified bridge from the MA to the pterygoids (PT) ventral to the BS. The cavum epiptericum is flattened such that its lateral wall and floor are less angled and more co-planar. The lamina obturans (LO) is less rectangular and more spade-like in shape. The associated foramina (e.g. ovale and rotundum) are displaced laterally. The rostral border of the LO is usually bifurcated, often with an ectopic flange and secondary cartilage (black arrowhead). Not surprisingly, this region supports anomalous muscle development (not shown). (I) The superior cornu (SC) of the thyroid cartilage (TC) fail to form in the mutants. Abbreviations: AP, angular process; AT, ala temporalis; BS, basisphenoid; BtP, basitrabecular process; CC, cricoid cartilage; CdP, condylar process; CrP, coronoid process; DNT, dentary; GV, trigeminal ganglion; GVII, facial ganglion; GVIII, acoustic ganglion; LO, lamina obturans; MA, malleus; MC, Meckel's cartilage; MF, mental foramen; OP, os paradoxicum; PT, pterygoid; SC, superior cornu of the thyroid cartilage; TC, thyroid cartilage; 1, ophthalmic branch of GV; 2, maxillary branch of GV; 3, mandibular branch of GV.

that the *Dlx* genes also cooperate to control craniofacial skeletogenesis (Qiu et al., 1997). The expression patterns of *Dlx1*, *Dlx2*, *Dlx3*, *Dlx5* and *Dlx6* suggest a model that may explain why the phenotypic effects of the *Dlx1* and *Dlx2* mutations are focused on skeletal elements derived from the proximal parts of the branchial arches (Fig. 7; Qiu et al., 1997). While *Dlx1* and *Dlx2* are expressed along most of the P/D axis of the first and second branchial arches, the expression of *Dlx3*, *Dlx5* and *Dlx6* is restricted to more distal regions (Fig. 7A). Thus, if the Dlx3, Dlx5 and Dlx6 proteins can compensate for the loss of Dlx1 and/or Dlx2, this could explain why mandibular and distal hyoid arches are not affected in the *Dlx1*, *Dlx2* and *Dlx1/2* mutants. The fact that the *Dlx1*, *Dlx2* and *Dlx1/2* mutants are not complete phenocopies could be due to

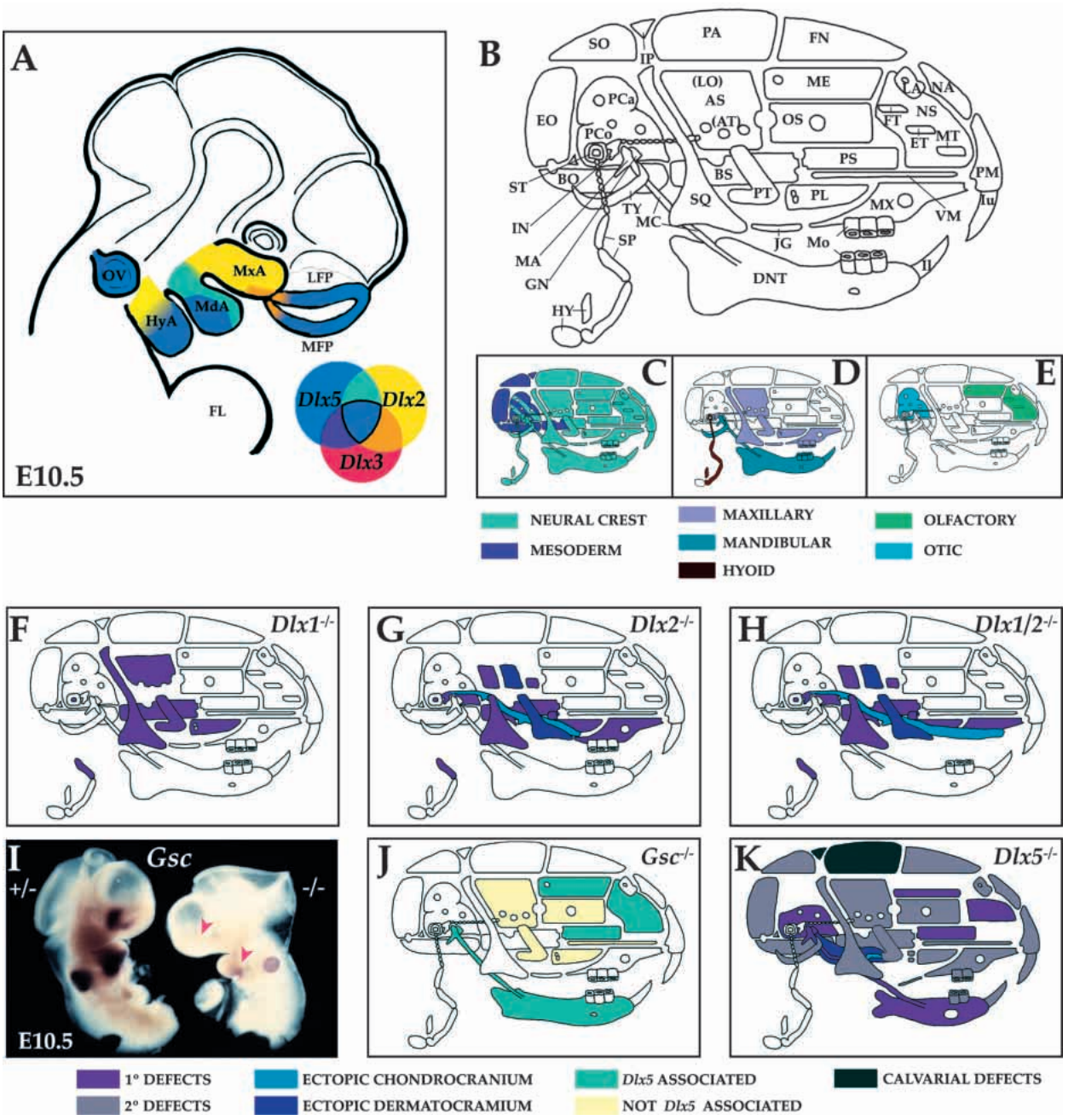

the following independent mechanisms: (1) the quantity of Dlx protein might be crucial, (2) *Dlx1* and *Dlx2* are not fully redundant, and (3) there is cross-regulation between *Dlx1* and *Dlx2*. Thus, each branchial arch may require both a threshold concentration of Dlx proteins as well as the unique properties of each protein. Mutation of *Dlx3*, *Dlx5* or *Dlx6* could therefore affect the mandibular and distal hyoid arches despite the potential compensatory presence of *Dlx1* and *Dlx2*.

In assessing this hypothesis, we analyzed the branchial-arch-derived skeleton in the *Dlx5* mutants, and found that the proximal end of Meckel's cartilage reorients and bifurcates just rostral to its connection with the malleus (Figs 6, 7K). The medial part of the bifurcation gives rise to a novel cartilage, which forms a strut that extends to the pterygoids. We have named this novel structure the os paradoxicum. It is curious that a strut also forms in the *Dlx2* and *Dlx1/2* mutants (Qiu et al., 1995, 1997). While the struts in the *Dlx2* and *Dlx5* mutants form in roughly the same rostrocaudal position, they are clearly distinct by virtue of their connections and their dorsoventral planes. In addition to proximal defects in the mandibular arch splanchnocranium, dermatocranial derivatives are dysmorphic, having unusual articulations and soft tissue connections. Unlike the *Dlx1*, *Dlx2* and *Dlx1/2* mutants, which have defects of the proximal skeleton of the hyoid arch, *Dlx5* mutants appear to have normal second arch cartilages. The fourth arch-derived superior cornu of the TC, however, fail to form. Thus, loss of Dlx5 is not fully compensated by the presence of other Dlx proteins. We are making compound mutants of *Dlx1*, *Dlx2*

Fig. 7. Schemata of *Dlx* gene expression at E10.5 and regional craniofacial defects in *Dlx* and *Gsc* mutations. (A) Schema depicting *Dlx*2, *Dlx3* and *Dlx5* expression in an E10.5 embryo. Overlapping expression of these genes is defined by the color wheel. *Dlx1* and *Dlx6* have similar expression patterns to *Dlx2* and *Dlx5*, respectively (Qiu et al., 1997). (B) Model of skeletal elements of the protovertebrate skull (after Flower, 1885; Broom, 1930). (C) Schema depicting the elements theoretically formed by CNC (green) or mesoderm (purple). (D) Elements from the maxillary (lavender) first arch, mandibular (blue) first arch and hyoid (brown) arch. (E) Elements with major contributions to the otic (blue) and nasal (green) capsules. (F) Elements altered in *Dlx1* mutants. It is suggested that elements having primary defects (in purple) are due to abnormalities in patterning. (G) Elements altered in *Dlx2* mutants. Those in light blue represent ectopic chondrocranial elements; those in dark blue represent ectopic dermatocranial elements. (H) Elements altered in *Dlx1/2* double mutants. (I) Whole-mount in situ hybridization of *Gsc* transcripts in heterozygote (left) and *Dlx5* mutant (right) E10.5 embryos. *Gsc* signal is reduced in the mesenchyme of the frontonasal prominences and in the mandibular and hyoid arch mesenchyme (red arrowheads). (J) Our interpretation of the reported *Gsc* mutant phenotype. Those elements in green have phenotypes similar to the *Dlx5* mutants. Elements in light yellow may not be linked to *Dlx5* function at E10.5. (K) Depiction of the elements altered by the loss of *Dlx5* expression. Primary defects defined as above. Elements with secondary defects are defined as those whose abnormalities may be due to defects in skeletal differentiation and/or to biomechanical effects. Hypomineralization defects of the parietal (PA) and interparietal (IP) are indicated in black. Change in elements within the nasal capsule and the mandible are hypothesized as due, in part, to a loss of *Gsc* expression. Abbreviations: AS, alisphenoid; AT, ala temporalis; BO, basioccipital; BS, basisphenoid; DNT, dentary; EO, exoccipital; ET, ethmoturbinate; FL, forelimb; FN, frontal; FT, frontoturbinate; GN, gonial; HY, hyoid; HyA, hyoid arch; Il, lower incisor; IN, incus; IP, interparietal; Iu, upper incisor; JG, jugal; LA, lachrimal; LFP, lateral frontonasal prominence; LO, lamina obturans; MA, malleus; MC, Meckel's cartilage; MdA, mandibular arch; ME, mesethmoid; MFP, medial frontonasal prominence; Mo, molars; MT, maxilloturbinate; MxA, maxillary arch; MX, maxilla; NA, nasal bone; NS, nasal septum; OC, otic capsule; OS, orbitosphenoid; OV, otic vesicle; PA, parietal; PCa, pars canalicularis; PCo, pars cochlearis; PL, palatine; PM, premaxilla; PS, presphenoid; PT, pterygoid; SO, supraoccipital; SP, styloid process; SQ, squamosal; ST, stapes; TY, tympanic; VM, vomer.

and *Dlx5* to further test predictions about the roles of each gene in patterning the branchial arch skeleton.

The *Dlx* genes have dynamic expression patterns and essential regulatory roles during tooth formation (Weiss et al., 1994, 1995, 1998; Qiu et al., 1997; Thomas et al., 1997, 1998). A frame-shift mutation in *DLX3* is associated with taurodontism and enamel hypoplasia in humans with Tricho-dento-osseous (TDO) syndrome (Price et al., 1998). TDO patients also have a thickening of the cranial bones. Moreover, the *Dlx1/2* double mutants lack maxillary molars (Qiu et al., 1997; Thomas et al., 1997). Unlike *Dlx1* and *Dlx2* single mutants, however, whose teeth appear to be normal, the *Dlx5* mutation affects, to varying degrees, development of all of the teeth (see results).

Decreased expression at E10.5 of *Gsc* suggests that *Dlx5* may function in one of several recently recognized pathways which appear to regulate *Gsc* expression. Current evidence suggests that *Gsc* expression is sensitive to signalling through both Fgf8 and endothelin-1 (ET-1) via its receptor, ET-A. For example, experimental evidence using mandibular arch ex vivo cultures has suggested that *Gsc* expression is either directly of indirectly inducible by Fgf8 (Tucker et al., 1999). Moreover, gene targetted loss of *ET-A* results in a loss of expression of *Gsc* within the first branchial arch (Clouthier et al., 1998). It remains to be determined if *Dlx5* mediates transcription of *Gsc* through either of these signalling systems.

Dlx1, *Dlx2* and *Dlx5* mutants have normal limbs

Dlx genes are also expressed in the apical ectodermal ridge of vertebrate limb buds (Dollé et al., 1992; Robinson and Mahon, 1994; Ferrari et al., 1995) and their invertebrate homologues are expressed in, and required for, developing appendages (Stock et al., 1996; Panganiban et al., 1997; Williams, 1998; Wu and Cohen, 1999). Thus, it is surprising that none of the reported *Dlx* mutants (*Dlx1*, *Dlx2*, *Dlx1/2* and here *Dlx5*) have obvious defects of limb development. The most-likely explanation is that of genetic compensation. In this regard, there is evidence implicating *DLX5* and *DLX6* in ectrodactyly in humans (Scherer et al., 1994; Crackower et al., 1996). Often, these patients also have cleft palate and deafness (Ignatius et al., 1996), defects that are consistent with the functions of *Dlx5* described herein. Thus, it would be instructive to study the limb phenotypes of *Dlx* compound mutants, particularly the *Dlx5/6* double mutants. In addition, people with ectrodactyly can have mental retardation (Ignatius et al., 1996). Perhaps this is due to the expression of *Dlx5* in the developing brain (Simeone et al., 1994; Liu et al., 1997).

M. J. D. would like to thank Dr Michael Novacek of the American Museum of Natural History, Dr Philip Crossley of the University of California, San Francisco, and Drs James Patton and David Wake, of the University of California, Berkeley, for their insightful comments. This work was supported by the research grants to J. L. R. R. from Nina Ireland, the March of Dimes, NARSAD, and NIH Grant MH51561 and K02 MH01046; to R. A. P. from NIH Grant HD26732, and United States Department of Energy /OHER Contract No. DE-ACO3-76-SF01012; and to M. J. D. from NIDR training grant T32 DE07204 and ARCS.

REFERENCES

Akimenko, M. A., Ekker, M., Wegner, J., Lin, W. and Westerfield, M. (1994) Combinatorial expression of three zebrafish genes related to distal-less: part of a homeobox gene code for the head. *J. Neurosci.* **14**, 3475-3486.

Anderson, S. A., Eisenstat, D. D., Shi, L. and Rubenstein, J. L. R. (1997a) Interneuron migration from basal forebrain to neocortex: dependence on Dlx genes. *Science* **278**, 474-476.

Anderson, S. A., Qiu, M., Bulfone, A., Eisenstat, D. D., Meneses, J., Pedersen, R. and Rubenstein, J. L. R. (1997b) Mutations of the homeobox genes Dlx-1 and Dlx-2 disrupt the striatal subventricular zone and differentiation of late born striatal neurons. *Neuron* **19**, 27-37.

Barghusen, H. R. and Hopson, A. (1979) The endoskeleton: The comparative anatomy of the skull and visceral skeleton. In *Hyman's Comparative Anatomy*. (ed. M. Wake) pp. 265-326. Chicago, IL: The University of Chicago Press.

Begbie, J., Brunet, J. F., Rubenstein, J. L. R. and Graham, A. (1999) Induction of the epibranchial placodes. *Development* **126**, 895-902.

Belo, J. A., Leyns, L., Yamada, G. and De Robertis, E. M. (1998) The prechordal midline of the chondrocranium is defective in Goosecoid-1 mouse mutants. *Mechan. Dev.* **72**, 15-25.

Broom, R. (1930) *The Origin of the Human Skeleton: an Introduction to Human Osteology*. London: H. F. & G. Witherby.

Bulfone, A., Puelles, L., Porteus, M. H., Frohman, M. A., Martin, G. R.

and Rubenstein, J. L. R. (1993) Spatially restricted expression of Dlx-1, Dlx-2 (Tes-1), Gbx-2, and Wnt-3 in the embryonic day 12. 5 mouse forebrain defines potential transverse and longitudinal segmental boundaries. *J. Neurosci.* **13**, 3155-3172.

Chen, X., Li, X., Wang, W. and Lufkin, T. (1996) Dlx5 and Dlx6: an evolutionary conserved pair of murine homeobox genes expressed in the embryonic skeleton. *Ann. New York Acad. Sci.* **785**, 38-47.

Clouthier, D. E., Hosoda, K., Richardson, J. A., Williams, S. C., Yanagisawa, H., Kuwaki, T., Kumada, M., Hammer, R. E. and Yanagisawa, M. (1998) Cranial and cardiac neural crest defects in endothelin-A receptor-deficient mice. *Development* **125**, 813-824.

Corsin, J. (1971) Influence des placodes olfactives et des ebauches optiques sur la morphagenese du squelette cranien chez *Pleurodeles waltii* michah. *Annales d'Embryologie et de morphogenese* **1**, 41-48.

Couly, G. F. and Le Douarin, N. M. (1985) Mapping of the early neural primordium in quail-chick chimeras. I. Developmental relationships between placodes, facial ectoderm, and prosencephalon. *Dev. Biol.* **110**, 422-439.

Couly, G. F. and Le Douarin, N. M. (1987) Mapping of the early neural primordium in quail-chick chimeras. II. The prosencephalic neural plate and neural folds: implications for the genesis of cephalic human congenital abnormalities. *Dev. Biol.* **120**, 198-214.

Couly, G. F., Coltey, P. M. and Le Douarin, N. M. (1993) The triple origin of skull in higher vertebrates: a study in quail-chick chimeras. *Development* **117**, 409-429.

Crackower, M. A., Scherer, S. W., Rommens, J. M., Hui, C. C., Poorkaj, P., Soder, S., Cobben, J. M., Hudgins, L., Evans, J. P. and Tsui, L. C. (1996) Characterization of the split hand/split foot malformation locus SHFM1 at 7q21. 3-q22. 1 and analysis of a candidate gene for its expression during limb development. *Human Molecular Genetics* **5**, 571-579.

Dattani, M. T., Martinez-Barbera, J. P., Thomas, P. Q., Brickman, J. M., Gupta, R., Mårtensson, I. L., Toresson, H., Fox, M., Wales, J. K., Hindmarsh, P. C., Krauss, S., Beddington, R. S. and Robinson, I. C. (1998) Mutations in the homeobox gene HESX1/Hesx1 associated with septo-optic dysplasia in human and mouse. *Nature Genetics* **19**, 125-133.

De Beer, G. (1985) *The Development of the Vertebrate Skull*. Chicago: Univeristy of Chicago Press.

Dollé, P., Price, M. and Duboule, D. (1992) Expression of the murine Dlx-1 homeobox gene during facial, ocular and limb development. *Differentiation* **49**, 93-99.

Eagleson, G., Ferreiro, B. and Harris, W. A. (1995) Fate of the anterior neural ridge and the morphogenesis of the Xenopus forebrain. *J. Neurobiol.* **28**, 146-158.

Eales, N. B. (1950) The skull of the foetal narwhal, *Monodon monoceros* L. *Phil. Trans. Roy. Soc. London, B* **235**, 1-33.

Ellies, D. L., Langille, R. M., Martin, C. C., Akimenko, M. A. and Ekker, M. (1997) Specific craniofacial cartilage dysmorphogenesis coincides with a loss of dlx gene expression in retinoic acid-treated zebrafish embryos. *Mech. Dev.* **61**, 23-36.

Ferrari, D., Sumoy, L., Gannon, J., Sun, H., Brown, A. M., Upholt, W. B. and Kosher, R. A. (1995) The expression pattern of the Distal-less homeobox-containing gene Dlx-5 in the developing chick limb bud suggests its involvement in apical ectodermal ridge activity, pattern formation, and cartilage differentiation. *Mech. Dev.* **52**, 257-264.

Flower, W. H. (1885) *An Introduction to the Osteology of the Mammalia*. London: Macmillan.

Francis-West, P., Ladher, R., Barlow, A. and Graveson, A. (1998) Signalling interactions during facial development. *Mech. Dev.* **75**, 3-28.

Frenz, D. A. and Van De Water, T. R. (1991) Epithelial control of periotic mesenchyme chondrogenesis. *Dev. Biol.* **144**, 38-46.

Fritzsch, B., Barald, K. F. and Lomax, M. I. (1998) Early embryology of the vertebrate ear. In *Development of the Auditory System*. (ed. E. W. Rubel, A. N. Proper and R. R. Fay). New York: Springer-Verlag.

Gaunt, S. J., Blum, M. and De Robertis, E. M. (1993) Expression of the mouse goosecoid gene during mid-embryogenesis may mark mesenchymal cell lineages in the developing head, limbs and body wall. *Development* **117**, 769-778.

Gendron-Maguire, M., Mallo, M., Zhang, M. and Gridley, T. (1993) Hoxa-2 mutant mice exhibit homeotic transformation of skeletal elements derived from cranial neural crest. *Cell* **75**, 1317-1331.

Goodrich, E. S. (1958) *Studies on the Structure and Development of Vertebrates*. New York: Dover Publications.

Grobstein, C. and Holtzer, H. (1955) 'In vitro' studies of cartilage induction in mouse somite mesoderm. *Exp. Zool.* **28**, 333-357.

Grüneberg, H. (1963). *The Pathology of Development: a study of inherited skeletal disorders in animals.* New York: John Wiley & Sons Inc.

Hall, B. K. (1988) *The Neural Crest*. Oxford University Press, London.

Hall, B. K. (1991) Cellular interactions during cartilage and bone development. *J. Craniofacial Genet. Dev. Biol.* **11**, 238-250.

Hanken, J. and Hall, B. K. (1993) Mechanisms of skull diversity and evolution. In *The Skull, Volume 3: Functional and Evolutionary Mechanisms*. (ed. J. Hanken and B. K. Hall). pp. 1-36. Chicago: University of Chicago Press.

Hanken, J. and Thorogood, P. (1993) Evolution and development of the vertebrate skull: the role of pattern formation. *Trends in Ecology & Evolution* **8**, 9-15.

Helms, J. A., Kim, C. H., Hu, D., Minkoff, R., Thaller, C. and Eichele, G. (1997) Sonic hedgehog participates in craniofacial morphogenesis and is down-regulated by teratogenic doses of retinoic acid. *Dev. Biol.* **187**, 25-35.

Hu, D. and Helms, J. A. (1999). Roles for Sonic Hedgehog in normal and abnormal craniofacial morphogenesis. *Development* (in press).

Ignatius, J., Knuutila, S., Scherer, S. W., Trask, B. and Kere, J. (1996) Split hand/split foot malformation, deafness, and mental retardation with a complex cytogenetic rearrangement involving 7q21. 3. *J. Med. Genet.* **33**, 507-510.

Imai, H., Osumi-Yamashita, N., Ninomiya, Y. and Eto, K. (1996) Contribution of early-emigrating midbrain crest cells to the dental mesenchyme of mandibular molar teeth in rat embryos. *Dev. Biol.* **176**, 151-165.

Jacobson, A. G. (1963) The determination and positioning of the nose, lens and ear. I. Interactions within the ectoderm, and between the ectoderm and underlying tissues. *J. Exp. Zool.* **154**, 273-284.

Jacobson, A. G. (1966) Inductive processes in embryonic development. *Science* **152**, 25-34.

Johnson, R. S., Sheng, M., Greenberg, M. E., Kolodner, R. D., Papaioannou, V. E. and Spiegelman, B. M. (1989) Targeting of nonexpressed genes in embryonic stem cells via homologous recombination. *Science* **245**, 1234-1236.

Joyner, A. L. (1993) *Gene Targeting: a Practical Approach*. Oxford: IRL Press at Oxford University Press.

Klima, M. (1987) Morphogenesis of the nasal structures of the skulls in toothed whales (Odontoceti). In *Morphogenesis of the Mammalian Skull*. (ed. H. Kuhn and U. Zeller), pp. 105-122. Hamburg: Verlag Paul Paray,

Köntges, G. and Lumsden, A. (1996) Rhombencephalic neural crest segmentation is preserved throughout craniofacial ontogeny. *Development* **122**, 3229-3242.

Kuratani, S., Matsuo, I. and Aizawa, S. (1997) Developmental patterning and evolution of the mammalian viscerocranium: genetic insights into comparative morphology. *Dev. Dynamics* **209**, 139-155.

Le Douarin, N. (1982) *The Neural Crest*. Cambridge Univeristy Press, London.

Legan, P. K. and Richardson, G. P. (1997) Extracellular matrix and cell adhesion molecules in the developing inner ear. *Seminars in Cell & Developmental Biology* **8**, 217-224.

Levin, M. and Mercola, M. (1998) The compulsion of chirality: toward an understanding of left-right asymmetry. *Genes Dev.* **12**, 763-769.

Liu, J. K., Ghattas, I., Liu, S., Chen, S. and Rubenstein, J. L. R. (1997) Dlx genes encode DNA-binding proteins that are expressed in an overlapping and sequential pattern during basal ganglia differentiation. *Dev. Dynamics* **210**, 498-512.

Lumsden, A. G. (1988) Spatial organization of the epithelium and the role of neural crest cells in the initiation of the mammalian tooth germ. *Development* **103 Supplement**, 155-169.

Matsuo, I., Kuratani, S., Kimura, C., Takeda, N. and Aizawa, S. (1995) Mouse Otx2 functions in the formation and patterning of rostral head. *Genes Dev.* **9**, 2646-2658.

McLeod, M. J. (1980) Differential staining of cartilage and bone in whole mouse fetuses by alcian blue and alizarin red S. *Teratology* **22**, 299-301.

Mina, M. and Kollar, E. J. (1987) The induction of odontogenesis in non-dental mesenchyme combined with early murine mandibular arch epithelium. *Arch. Oral Biol.* **32**, 123-127.

Moore, W. J. (1981) *The Mammalian Skull*. Cambridge University Press, Cambridge.

Neubüser, A., Peters, H., Balling, R. and Martin, G. R. (1997) Antagonistic interactions between FGF and BMP signaling pathways: a mechanism for positioning the sites of tooth formation. *Cell* **90**, 247-255.

Newberry, E. P., Latifi, T. and Towler, D. A. (1998) Reciprocal regulation

of osteocalcin transcription by the homeodomain proteins Msx2 and Dlx5. *Biochemistry* **37**, 16360-16368.

Noden, D. M. (1983) The role of the neural crest in patterning of avian cranial skeletal, connective, and muscle tissues. *Dev. Biol.* **96**, 144-165.

Noden, D. M. (1991) Vertebrate craniofacial development: the relation between ontogenetic process and morphological outcome. *Brain, Behavior and Evolution* **38**, 190-225.

Novacek, M. J. (1993) Patterns of diversity in the mammalian skull. In *The Skull, Volume 2: Patterns of Structural and Systematic Diversity*. (ed. J. Hanken and B. K. Hall), pp. 438-545. Chicago: University of Chicago Press.

Osumi-Yamashita, N., Kuratani, S., Ninomiya, Y., Aoki, K., Iseki, S., Chareonvit, S., Doi, H., Fujiwara, M., Watanabe, T. and Eto, K. (1997) Cranial anomaly of homozygous rSey rat is associated with a defect in the migration pathway of midbrain crest cells. *Development, Growth and Differentiation* **39**, 53-67.

Osumi-Yamashita, N., Ninomiya, Y., Doi, H. and Eto, K. (1994) The contribution of both forebrain and midbrain crest cells to the mesenchyme in the frontonasal mass of mouse embryos. *Dev. Biol.* **164**, 409-419.

Panganiban, G., Irvine, S. M., Lowe, C., Roehl, H., Corley, L. S., Sherbon, B., Grenier, J. K., Fallon, J. F., Kimble, J., Walker, M., Wray, G. A., Swalla, B. J., Martindale, M. Q. and Carroll, S. B. (1997) The origin and evolution of animal appendages. *Proc. Nat. Acad. Sci. USA* **94**, 5162-5166.

Patten, B. M. and Carlson, B. M. (1988) *Patten's Foundations of Embryology*. New York: McGraw-Hill.

Price, J. A., Bowden, D. W., Wright, J. T., Pettenati, M. J. and Hart, T. C. (1998) Identification of a mutation in DLX3 associated with tricho-dento-osseous (TDO) syndrome. *Human Molecular Genetics* **7**, 563-569.

Qiu, M., Bulfone, A., Ghattas, I., Meneses, J. J., Christensen, L., Sharpe, P. T., Presley, R., Pedersen, R. A. and Rubenstein, J. L. R. (1997) Role of the Dlx homeobox genes in proximodistal patterning of the branchial arches: mutations of Dlx-1, Dlx-2, and Dlx-1 and -2 alter morphogenesis of proximal skeletal and soft tissue structures derived from the first and second arches. *Dev. Biol.* **185**, 165-184.

Qiu, M., Bulfone, A., Martinez, S., Meneses, J. J., Shimamura, K., Pedersen, R. A. and Rubenstein, J. L. R. (1995) Null mutation of Dlx-2 results in abnormal morphogenesis of proximal first and second branchial arch derivatives and abnormal differentiation in the forebrain. *Genes Dev.* **9**, 2523-2538.

Ramsdell, A. F. and Yost, H. J. (1998) Molecular mechanisms of vertebrate left-right develoment. *Trends in Genetics* **14**, 459-464.

Raven, H. C. and Gregory, W. K. (1933) The spermaceti organ and nasal passages of the sperm whale (*Physeter catodon*) and other odontocetes. *American Museum Novitates* **677**, 1-18.

Rijli, F. M., Gavalas, A. and Chambon, P. (1998) Segmentation and specification in the branchial region of the head: the role of the Hox selector genes. *Int. J. Dev. Biol.* **42**, 393-401.

Rijli, F. M., Mark, M., Lakkaraju, S., Dierich, A., Dolle, P. and Chambon, P. (1993) A homeotic transformation is generated in the rostral branchial region of the head by disruption of Hoxa-2, which acts as a selector gene. *Cell* **75**, 1333-1349.

Rivera-Pérez, J. A., Mallo, M., Gendron-Maguire, M., Gridley, T. and Behringer, R. R. (1995) Goosecoid is not an essential component of the mouse gastrula organizer but is required for craniofacial and rib development. *Development* **121**, 3005-3012.

Robinson, G. W. and Mahon, K. A. (1994) Differential and overlapping expression domains of Dlx-2 and Dlx-3 suggest distinct roles for Distal-less homeobox genes in craniofacial development. *Mech. Dev.* **48**, 199-215.

Rubenstein, J. L. R., Shimamura, K., Martinez, S. and Puelles, L. (1998) Regionalization of the prosencephalic neural plate. *Ann. Review Neurosci.* **21**, 445-477.

Ryoo, H. M., Hoffmann, H. M., Beumer, T., Frenkel, B., Towler, D. A., Stein, G. S., Stein, J. L., van Wijnen, A. J. and Lian, J. B. (1997) Stage-specific expression of Dlx-5 during osteoblast differentiation: involvement in regulation of osteocalcin gene expression. *Molec. Endocrin.* **11**, 1681-1694.

Sambrook, J., Maniatis, T. and Fritsch, E. F. (1989) *Molecular Cloning: a Laboratory Manual*. Cold Spring Harbor, NY: Cold Spring Harbor Laboratory.

Scherer, S. W., Poorkaj, P., Massa, H., Soder, S., Allen, T., Nunes, M., Geshuri, D., Wong, E., Belloni, E., Little, S. and et al. (1994) Physical mapping of the split hand/split foot locus on chromosome 7 and implication in syndromic ectrodactyly. *Human Molecular Genetics* **3**, 1345-1354.

Serbedzija, G. N., Bronner-Fraser, M. and Fraser, S. E. (1992) Vital dye analysis of cranial neural crest cell migration in the mouse embryo. *Development* **116**, 297-307.

Sher, A. E. (1971) The embryonic and postnatal development of the inner ear of the mouse. *Acta oto-Laryngologica* **Suppl. 285**, 1-77.

Shimamura, K., Hartigan, D. J., Martinez, S., Puelles, L. and Rubenstein, J. L. R. (1995) Longitudinal organization of the anterior neural plate and neural tube. *Development* **121**, 3923-3933.

Shimamura, K. and Rubenstein, J. L. R. (1997) Inductive interactions direct early regionalization of the mouse forebrain. *Development* **124**, 2709-2718.

Simeone, A., Acampora, D., Pannese, M., D'Esposito, M., Stornaiuolo, A., Gulisano, M., Mallamaci, A., Kastury, K., Druck, T., Huebner, K. and et al. (1994) Cloning and characterization of two members of the vertebrate Dlx gene family. *Proc. Nat. Acad. Sci. USA* **91**, 2250-2254.

Stock, D. W., Ellies, D. L., Zhao, Z., Ekker, M., Ruddle, F. H. and Weiss, K. M. (1996) The evolution of the vertebrate Dlx gene family. *Proc. Nat. Acad. Sci. USA* **93**, 10858-10863.

Thesleff, I. and Sharpe, P. (1997) Signalling networks regulating dental development. *Mech. Dev.* **67**, 111-123.

Thesleff, I., Vaahtokari, A. and Partanen, A. M. (1995) Regulation of organogenesis. Common molecular mechanisms regulating the development of teeth and other organs. *Int. J. Dev. Biol.* **39**, 35-50.

Thomas, B. L., Tucker, A. S., Ferguson, C., Qiu, M., Rubenstein, J. L. R. and Sharpe, P. T. (1998) Molecular control of odontogenic patterning: positional dependent initiation and morphogenesis. *Eur. J. Oral Sci.* **106 Suppl 1**, 44-47.

Thomas, B. L., Tucker, A. S., Qui, M., Ferguson, C. A., Hardcastle, Z., Rubenstein, J. L. R. and Sharpe, P. T. (1997) Role of Dlx-1 and Dlx-2 genes in patterning of the murine dentition. *Development* **124**, 4811-4818.

Thorogood, P. (1988) The developmental specification of the vertebrate skull. *Development* **103 Supplement**, 141-153.

Thorogood, P. (1993) Differentiation and morphogenesis of cranial skeletal tissues. In, *The Skull, Volume 1: Development*. (ed. J. Hanken and B. K. Hall). pp. 112-152. Chicago: University of Chicago Press.

Torres, M. and Giraldez, F. (1998) The development of the vertebrate inner ear. *Mech. Dev.* **71**, 5-21.

Tosney, K. W. (1982) The segregation and early migration of cranial neural crest cells in the avian embryo. *Dev. Biol.* **89**, 13-24.

Tucker, A. S., Matthews, K. L. and Sharpe, P. T. (1998) Transformation of tooth type induced by inhibition of BMP signaling. *Science* **282**, 1136-1138.

Tucker, A. S., Yamada, G., Grigoriou, M., Pachnis, V. and Sharpe, P. T. (1999) Fgf-8 determines the rostral-caudal polarity in the first branchial arch. *Development* **51**, 51-61.

Tybulewicz, V. L., Crawford, C. E., Jackson, P. K., Bronson, R. T. and Mulligan, R. C. (1991) Neonatal lethality and lymphopenia in mice with a homozygous disruption of the c-abl proto-oncogene. *Cell* **65**, 1153-1163.

Van de Water, T. R. (1984) Developmental mechanisms of mammalian inner ear formation. In Berlin, C. I. (ed.) *Hearing Science: Recent Advances*. San Diego: Collage Hill Press.

Van de Water, T. R. and Galinovic-Schwartz, V. (1987) Collagen type II in the otic extracellular matrix. Effect on inner ear development. *Hearing Research* **30**, 39-47.

Verwoerd, C. and van Oostrom, C. (1979) Cephalic neural crest and placodes. *Advances in Anatomy, Embryology, and Cell Biology* **58**, 1-71.

Webb, J. F. and Noden, D. M. (1993) Ectodermal placodes: Contributions to the development of the vertebrate head. *American Zoologist* **33**, 434-447.

Weiss, K. M., Bollekens, J., Ruddle, F. H. and Takashita, K. (1994) Distal-less and other homeobox genes in the development of the dentition. *J. Exp. Zool.* **270**, 273-284.

Weiss, K. M., Ruddle, F. H. and Bollekens, J. (1995) Dlx and other homeobox genes in the morphological development of the dentition. *Connective Tissue Research* **32**, 35-40.

Weiss, K. M., Stock, D., Zhao, Z., Buchanan, A., Ruddle, F. and Shashikant, C. (1998) Perspectives on genetic aspects of dental patterning. *Eur. J. Oral Sci.* **106 Suppl 1**, 55-63.

White, T. D. and Folkens, P. A. (1991) *Human Osteology*. San Diego: Academic Press.

Williams, T. A. (1998) Distalless expression in crustaceans and patterning of branched limbs. *Development, Genes and Evolution* **207**, 427-434.

Wu, J. and Cohen, S. M. (1999) Proximodistal axis formation in the Drosophila leg: subdivision into proximal and distal domains by Homothorax and Distal-less. *Development* **126**, 109-117.

Xu, C., Harris, A., lefebvre, V., de Crombrugghe, B., Rubenstein, J. L. R., Mundy, G. R. and Harris, S. E. (1999) Homeobox gene Dlx-2 is required

for Bone Morphogenetic Protein-2 (BMP2) signalling to the Pro-alpha1 (II) Collagen in chondroblasts. *Molecular Endocrinology* **in press**.

Yamada, G., Mansouri, A., Torres, M., Stuart, E. T., Blum, M., Schultz, M., De Robertis, E. M. and Gruss, P. (1995) Targeted mutation of the murine goosecoid gene results in craniofacial defects and neonatal death. *Development* **121**, 2917-2922.

Yamada, G., Ueno, K., Nakamura, S., Hanamure, Y., Yasui, K., Uemura, M., Eizuru, Y., Mansouri, A., Blum, M. and Sugimura, K. (1997) Nasal and pharyngeal abnormalities caused by the mouse goosecoid gene mutation. *Biochem. Biophys. Res. Commun.* **233**, 161-165.

Yang, L., Zhang, H., Hu, G., Wang, H., Abate-Shen, C. and Shen, M. M. (1998) An early phase of embryonic Dlx5 expression defines the rostral boundary of the neural plate. *J. Neurosci.* **18**, 8322-8330.

Youssef, E. H. (1966) The chondrocranium of the albino rat. *Acta Anatomica* **64**, 586-617.

Zeller, U. (1987) Morphogenesis of the mammalian skull with special reference to *Tupaia*. In *Morphogenesis of the Mammalian Skull* (ed. H. Kuhn and U. Zeller). pp. 17-50. Hamburg: Verlag Paul Paray.

Zhao, G. Q., Zhao, S., Zhou, X., Eberspaecher, H., Solursh, M. and de Crombrugghe, B. (1994) rDlx, a novel distal-less-like homeoprotein is expressed in developing cartilages and discrete neuronal tissues. *Dev. Biol.* **164**, 37-51.